AD-A125 277 COMPUTER BASED METHODS FOR THERMODYNAMIC ANALYSIS OF 1/1
MATERIALS PROCESSING(U) MANLABS INC CAMBRIDGE MASS
L KAUFMAN ET AL. 02 NOV 82 AFOSR-TR-83-1094
UNCLASSIFIED F49620-80-C-0020 F/G 9/2 NL

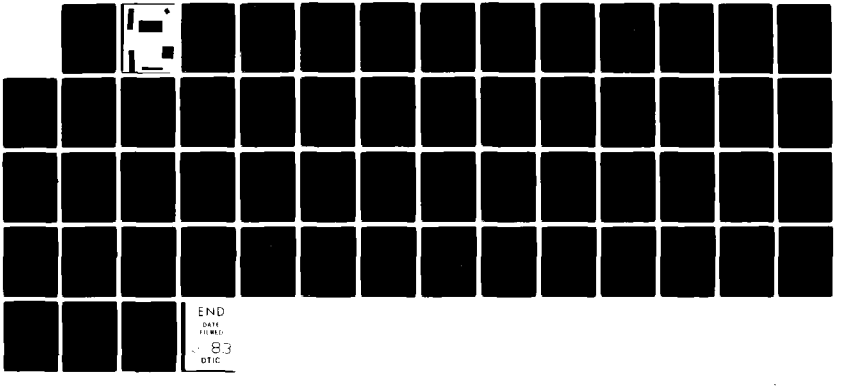

END
DATE FILMED
83
DTIC

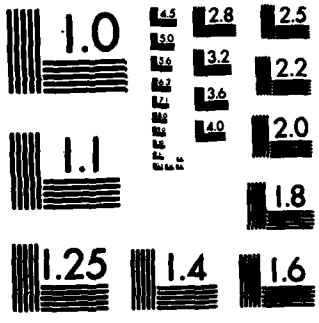

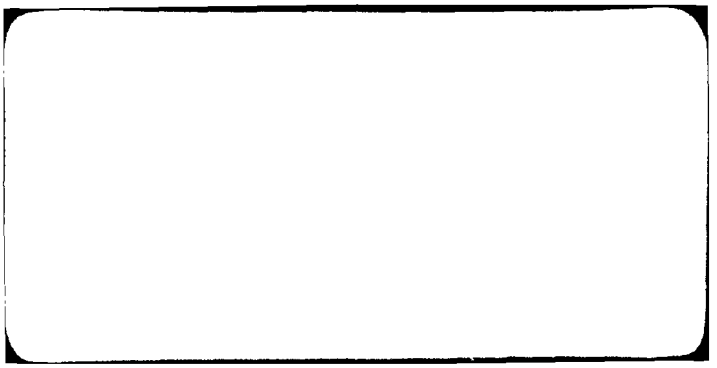

(13)

Annual Report

on

CONTRACT F 49620-80-C-0020
AFOSR-TR- 82-1094
COMPUTER BASED METHODS
FOR THERMODYNAMIC ANALYSIS
OF MATERIALS PROCESSING
1 October 1981 to 30 September 1982

Submitted to

Air Force Office of Scientific Research
(AFSC)
Bolling Air Force Base, D.C. 20332

2 November 1982

by

Larry Kaufman and John Agren

ManLabs, Inc.
21 Erie Street
Cambridge, Massachusetts 02139

UNCLASSIFIED

SECURITY CLASSIFICATION OF THIS PAGE (When Data Entered)

REPORT DOCUMENTATION PAGE	READ INSTRUCTIONS BEFORE COMPLETING FORM
1. REPORT NUMBER: AFOSR-TR- 82-1094 2. GOVT ACCESSION NO.: AD-A1252 77	3. RECIPIENT'S CATALOG NUMBER
4. TITLE (and Subtitle): Computer Based Methods for Thermodynamic Analysis of Materials Processing	5. TYPE OF REPORT & PERIOD COVERED: Annual Report 1 Oct. 1981 to 30 Sept. 1982 6. PERFORMING ORG. REPORT NUMBER
7. AUTHOR(s): Larry Kaufman and John Agren	8. CONTRACT OR GRANT NUMBER(s): F 49620-80-C-0020
9. PERFORMING ORGANIZATION NAME AND ADDRESS: ManLabs Inc. 21 Erie St. Cambridge, Massachusetts 02139	10. PROGRAM ELEMENT, PROJECT, TASK AREA & WORK UNIT NUMBERS: 61102F 2306/A2
11. CONTROLLING OFFICE NAME AND ADDRESS: Air Force Office of Scientific Research AFSC Bolling Air Force Base, D.C. 20332	12. REPORT DATE: 2 November 1982 13. NUMBER OF PAGES: 53
14. MONITORING AGENCY NAME & ADDRESS (if different from Controlling Office)	15. SECURITY CLASS. (of this report): Unclassified 15a. DECLASSIFICATION DOWNGRADING SCHEDULE

16. DISTRIBUTION STATEMENT (of this Report)

Approved for public release; distribution unlimited.

17. DISTRIBUTION STATEMENT (of the abstract entered in Block 20, if different from Report)

18. SUPPLEMENTARY NOTES

19. KEY WORDS (Continue on reverse side if necessary and identify by block number)

Data Base	Quasi Teunary	Hard metal coatings
Phase Diagrams	Iron base Alloys	Chemical Vapor Deposition
Fluoride Gases	Ordering Reactions	Titonium Carbo-Nitrides
Quasi Binary	Thermochemical Properties	

20. ABSTRACT (Continue on reverse side if necessary and identify by block number)

A data base is being developed for calculating binary, ternary and multi component phase diagrams for systems of interest in processing novel materials. Current applications cover Zirconium Fluoride based Glasses for tunable gap Electro-Optical applications, Iron-Aluminum based alloys for high temperature applications and titonium-carbo-nitride compounds for hard metal coatings.

A

DD FORM 1 JAN 73 1473 EDITION OF 1 NOV 65 IS OBSOLETE

Unclassified

SECURITY CLASSIFICATION OF THIS PAGE (When Data Entered)

Abstract

The recent discovery of a new family of non-oxide glasses based on mixtures of ZrF_4 or HfF_4 with other metallic fluorides by M. Poulain and coworkers offers great potential in optical fiber, window and source/detector application. Due to the limited phase diagram data available for the binary, ternary and multicomponent fluoride systems currently employed to synthesize these glasses most of the progress in identifying new compositions has proceeded along empirical lines. The data base developed for fluoride systems has been expanded and employed to calculate the composition of maximum liquid stability in the ZrF_4-LaF_3-BaF_2 and the ZrF_4-BaF-NaF ternary systems where glass formation has been observed. Recalculation of the fcc/bcc equilibria in the iron- aluminum-maganese systems at high temperatures in order to reflect the specific effects of ordering in the bcc phase does not produce any substantial changes in comparison with earlier results obtained without specific consideration of ordering. An analysis of the titanium-carbon-nitrogen system coupling the thermochemical and phase diagram data has been performed to permit calculation of the ternary phase diagram and thermochemical properties over a range of temperature. This information should be useful in vapor deposition of coatings based on this system which are used in metal cutting and wear resistance applications.

I. PROGRESS DURING THE CURRENT YEAR

1. Calculation of Ternary Fluoride Glass Compositions

The recent discovery of a new family of non-oxide glasses based on mixtures of ZrF_4 or HfF_4 with other metallic fluorides by M. Poulain and coworkers offers great potential in optical fiber, window and source/detector application. Due to the limited phase diagram data available for the binary, ternary and multicomponent fluoride systems currently employed to synthesize these glasses most of the progress in identifying new compositions has proceeded along empirical lines. In order to remedy this situation, the development of a data base covering fluoride glasses has been undertaken. Coupled thermochemical analysis of the ZrF_4-BaF_2, ZrF_4-LaF_3, ZrF_4-PbF_2, ZrF_4-NaF, ZrF_4-KF, ZrF_4-RbF and ZrF_4-CsF, LaF_3-BaF_2 and BaF_2-NaF systems was completed. The results were employed to calculate the composition of maximum liquid stability in the ZrF_4-LaF_3-BaF_2 and the ZrF_4-BaF_2-NaF ternary systems where glass formation has been observed. Technical presentation of this material has been made at the AFOSR sponsored International Symposium on Halide and Non-Oxide Glasses and at CALPHAD XI at Argonne National Laboratory. A paper covering the details of the data base structure is presently being prepared for publication in the CALPHAD journal. A summary of the results is shown in Section IV on pages 4-6 of this report.

2. Calculation of the Effects of Ordering Reactions on the FCC/BCC Equilibria in Iron-Aluminum-Based Ternary Alloys

In the previous annual report the ManLabs Data Bank was employed to compute the effect of nickel and maganese additions on the fcc/bcc equilibrium in iron-aluminum alloys for use as high temperature engine components. The calculations reported were performed without specific concern for ordering in the bcc phase. Section V pages 7-26 contains an analysis of the ordering reactions in the iron-aluminum system and a recalculation of the fcc/bcc equilibria in

iron-aluminum-manganese and iron-aluminum-nickel alloys. The conclusion of these calculations is that specific consideration of the ordering effects do not materially alter the results reported previously.

3. Thermodynamic Evaluation of the Titanium-Carbon-Nitrogen Phase Diagram

Vapor deposited titanium carbide, titanium nitride and titanium carbo nitride are finding extensive use in metal cutting and wear resistance applications. An analysis of the titanium-carbon-nitrogen system detailed in Section VI on pages 27-52 couples the limited binary phase diagram data and thermochemistry in order to provide calculated ternary sections and chemical activity information for a wide range of temperatures.

II. PROGRAM PERSONNEL

Technical activities during the past year have been carried out by L. Kaufman, J. Agren, F. Hayes, D. Birney, J. Nell, E.P. Warekois, S. Sprung, S. Drake and C. Biddell of ManLabs, Inc.

III. TECHNICAL LECTURES

Technical lectures covering various aspects of the work conducted under this program have been presented at the International Symposium on Halide and Non-Oxide Glasses, Cambridge, England March 1982, CALPHAD XI, Argonne National Laboratory May 1982 and the Alloy Workshop , Los Alamos National Laboratory, September 1982.

IV. CALPHAD CALCULATION OF TERNARY FLUORIDE GLASS COMPOSITIONS*

L. Kaufman, J. Agren, J. Nell and F. Hayes
ManLabs, Inc. 21 Erie St., Cambridge, Mass. 02139 USA

The recent discovery of a new family of non-oxide glasses based on mixtures of ZrF_4 or HfF_4 with other metallic fluorides by M. Poulain and coworkers offers great potential in optical fiber, window and source/detector application. Due to the limited phase diagram data available for the binary, ternary and multicomponent fluoride systems currently employed to synthesize these glasses most of the progress in identifying new compositions has proceeded along empirical lines. In order to remedy this situation, the CALPHAD method (1-3) for coupling phase diagram and thermochemical data has been applied to develop a data base covering metallic fluorides. The objective is to permit computation of multicomponent phase diagrams which can be used to identify the composition range where the liquid is most stable. The latter offers opportunities for glass formation as demonstrated by predictions of new metallic glasses. Currently the data base covers combinations of 0.2 ZrF_4(ZF), 0.25 LaF_3(LF), 0.333 BaF_2(BF), 0.333 PbF_2(PF), 0.5 NaF(NF), 0.5 RbF(RF), 0.5 CsF(CF) and 0.5 KF(KF) which have been developed along the lines described earlier for III-V, II-VI and SIALON systems (2-3). Figures 1 and 2 and the accompanying tabular material show how the computed liquidus contours in LF-ZF-BF and BF-ZF-NF disclose the range of composition in which the liquid has the greatest stability. These compositions agree well with those in which Poulain and coworkers have discovered glass formation (4,5).

---

*This work has been sponsored by the Air Force Office of Scientific Research, Bolling Field, D.C. under AF4962-80-C-0020.

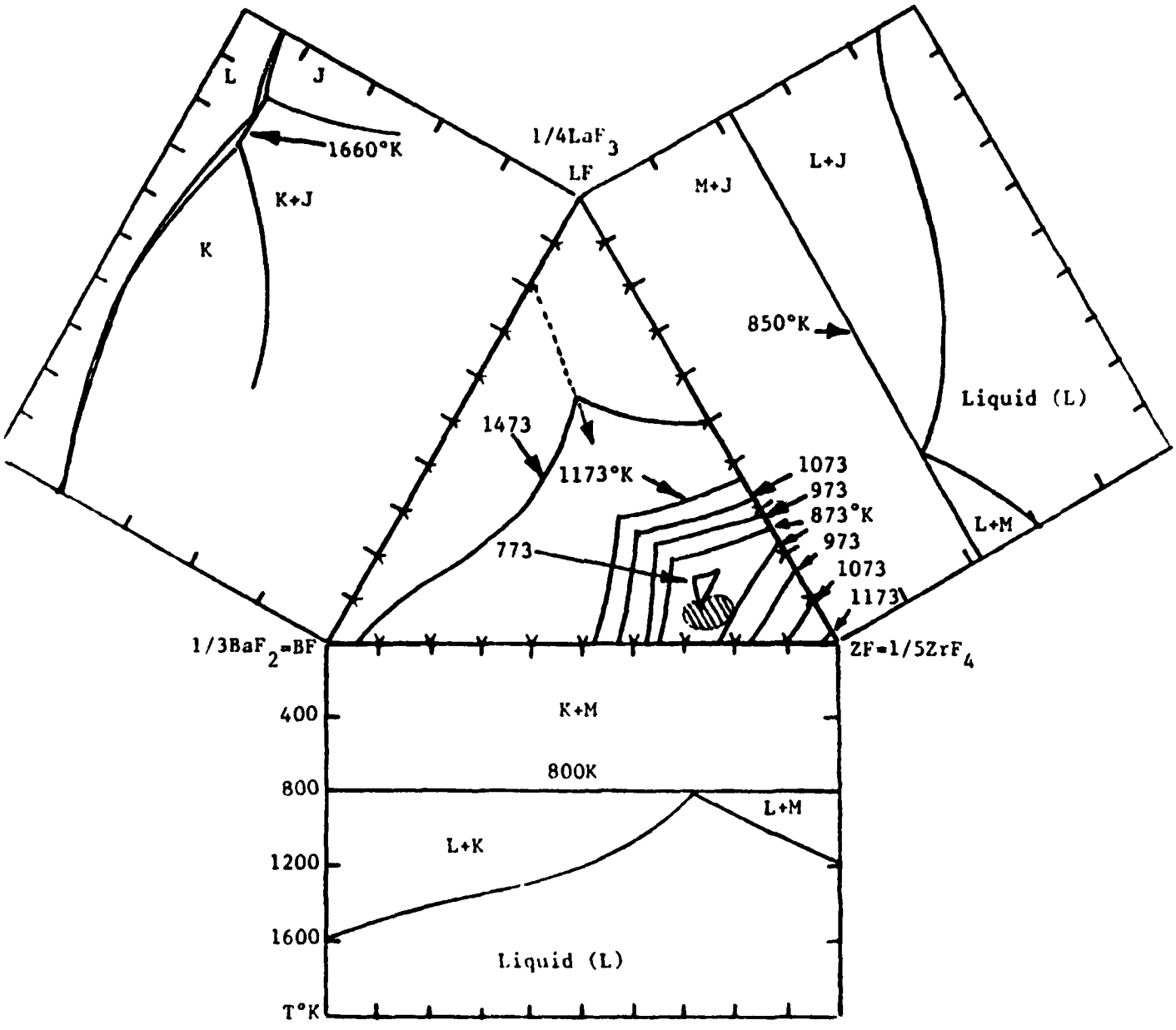

Figure 1. Calculated Edge Binary Systems and Liquidus Projections in the LF-ZF-BF System. The hatched region in the ternary denotes the glass forming composition range established experimentally by Lecoq and Poulaine (4).

SUMMARY OF LATTICE STABILITY, SOLUTION AND COMPOUND PARAMETERS, J/g.at., K

ZFZFLM=12845-10.67T, BFBFLK=9481-6.07T, LLFBF=21757-6.82T, LLFZF-22594, LZFLF=-11088
ZFZFLJ= -7.11T, BFBFLJ=8786-7.11T, LBFLF=21757-6.82T, LZFBF=-10155, LBFZF=-18271
ZFZFLK= -6.07T, BFBFLM= -10.67T,JLFBF=33137-12.55T,LBFNF=16736, LNFBF=12552
ZFZFLS= -11.97T, NFNFLS=16799-13.26T, JBFLF=33137-12.55T, LZFNF= -54392+29.29T
LFLFLJ=12560-7.11T, NFNFLK= -6.07T, KLFBF=25104-12.55T, LNFZF=-29288+29.29T
LFLFLM= -10.67T, NFNFLJ= -7.11T, KBFLF=25104-12.55T, MZFNF=MNFZF=SZFNF=SNFZF=2097
LFLFLK= -6.07T, NFNFLM= -10.67T, JLFZF=JZFLF=MLFZF=MZFLF=KBFLF=KLFBF=41840
KBFNF=KNFBF=SBFNF=SNFBF=41840; COMPOUND P, $NF_{0.286}ZF_{0.714}$, Base M, C=-17573+41.21T

COMPOUND Q, $NF_{0.545}ZF_{0.455}$, Base M, C=1912+43.01T, COMPOUND Q, $BF_{0.545}ZF_{0.455}$, Base M, C=33472

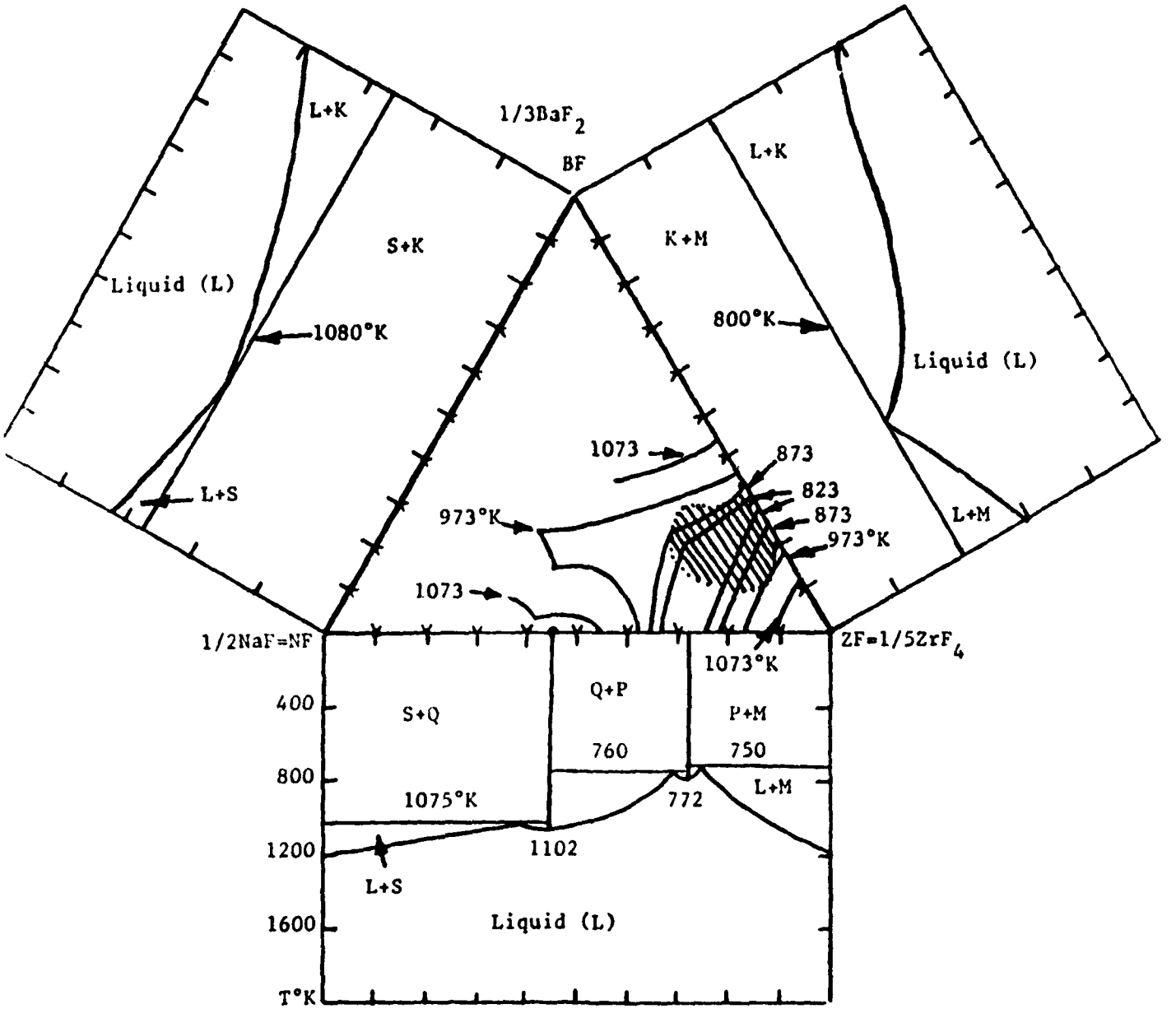

Figure 2. Calculated Edge Binary Systems and Liquidus Projections in the BF-ZF-NF System. The hatched region in the ternary denotes the glass forming composition range established experimentally by M. Poulain, M. Poulain and J. Lucas (5).

References

1. L. Kaufman, CALPHAD (1977) 1 14.
2. L. Kaufman, F. Hayes and D. Birnie, CALPHAD (1981) 5 163.
3. L. Kaufman, J. Nell, K. Taylor and F. Hayes, CALPHAD (1981) 5 185.
4. A. Lecoq and M. Poulain, J. Non-Crystalline Solids (1979) 34 101.
5. M. Poulain, M. Poulain and J. Lucas, Rev. de Chem. Mineral (1979) 16 267.

V. A SIMPLIFIED TREATMENT OF THE THERMODYNAMICS OF THE ORDER/DISORDER REACTIONS IN THE FE - Al SYSTEM

JOHN AGREN

Abstract

The Gibbs energy difference between ordered and disordered bcc phase in the Fe - Al system is presented as an explicit expression of composition. A power series expansion based on the shape of the Cp-curve is used. The thermodynamics of the Fe - Al phase diagram is evaluated and the diagram is calculated with the new model for the bcc phase. The Fe - Al - Mn and Fe - Al - Ni ternaries are calculated applying a subregular approximation of the new series-expansion. The deviations from previous calculations where no distinction between ordered and disordered bcc was made, are found to be very small.

A Simplified Treatment of the Thermodynamics of the Order/Disorder Reactions in the Fe-Al Phase Diagram

1. Introduction

It is well known that different types of ordering (i.e. magnetic or chemical) contribute considerably to the thermodynamic properties of a solid solution. Consequently the corresponding phase diagram might be strongly affected by the occurance of ordering. Inden (1) has presented extensive theoretical analyses of the order/disorder reactions in binary alloys. In a disordered, random solution the Bragg-Williams approximation and different regular solution models yield the Gibbs energy as a simple algebraic function of the composition of the solution. In a partially ordered phase the simple models also predict a dependence of the degree of order on composition and temperature. The most stable state of ordering for a certain composition and temperature is then the one that yields the lowest Gibbs energy. Thus it is not possible to write the Gibbs energy simply as an explicit function of the composition. In many applications it is desirable to express the Gibbs energy as a explicit function of composition. Inden (2) has presented a method where the ordering contribution to Gibbs energy is expanded in a power series of the temperature. The coefficients are functions of composition and adjusted to fulfill certain criteria. In the present work a slightly different method will be applied to the Fe-Al system. The method is based on the work by Inden (3) and has recently been applied to the magnetic ordering in alloys (4). The purpose of the present work is to show how the order/disorder reactions can be incorporated in a Calphad framework without an undue increase in complexity.

2. The Model

The integral molar Gibbs energy, G_m, of a phase can be separated into two parts.

$$G_m = G_m^{dis} + (G_m - G_m^{dis}) \qquad (1)$$

The first term G_m^{dis} is the Gibbs energy for the completely disordered state and is obtained from a regular solution type of model, i.e. --

$$G_m^{dis} = X_{Fe}{}^oG_{Fe} + X_{Al}{}^oG_{Al} + RT\left(X_{Fe}\ln X_{Fe} + X_{Al}\ln X_{Al}\right) + X_{Fe}X_{Al}L_{FeAl} \quad (2)$$

where L_{FeAl} is a constant for a regular solution and exhibits a linear concentration dependency in the subregular case. ${}^oG_{Fe}$ and ${}^oG_{Al}$ are the Gibbs energies for the pure elements for the structure considered.

The second term will now be evaluated by a method which has been applied to the magnetic ordering in bcc-Fe (4,5,6), and is a modification of a method initially proposed by Inden(3). Inden found that the following expressions gave an adequate description of the contribution from order/disorder reactions to the specific heat c_p,

$$\Delta c_p^{\alpha} = k^{\alpha}R\ln\frac{(1+\tau^3)}{(1-\tau^3)} \qquad \tau < 1 \quad (3a)$$

$$\Delta c_p^{\beta} = k^{\beta}R\ln\frac{(\tau^5+1)}{(\tau^5-1)} \qquad \tau > 1 \quad (3b)$$

where $\tau = T/T_C$, T_C being the critical temperature where all long range order vanishes. The superscripts α and β denote the states with long range order and short range order respectively, and, k^{α} and k^{β} are constants. By applying the first three terms in the Mc Laurin series expansion of Eq. 3, and integrating from $T=\infty$, where $G^{\beta} = G^{dis}$, to obtain the corresponding enthalpy and entropy, we can write down the expression for the Gibbs energy. It is convenient to express k^{β} and k^{α} in terms of the enthalpy difference between the ordered and the completely disordered state at 0 K, because this quantity is easy to obtain by counting the number of different bonds. By introducing f as the fraction of total enthalpy that is absorbed above T_C (i.e., f=0 when there is no short range ordering above T_C and the total enthalpy is then due to long range ordering only). We obtain:

$$-RT_C\,k^{\beta} = \frac{140}{79}\,f\,\Delta H_{T=0}^{dis \rightarrow ord} \quad (4a)$$

$$-RT_C\,k^{\alpha} = \frac{120}{71}\,(1-f)\,\Delta H_{T=0}^{dis \rightarrow ord} \quad (4b)$$

Inden (7) suggests that f=0.4 should be used for bcc-phases in general. By inserting Eq. 4 in our expression for $G_m - G_m^{dis}$ and setting f=0.4 we obtain:

$$G_m - G_m^{dis} = \Delta H_{T=0}^{dis \rightarrow ord} \; I(\tau) \tag{5}$$

where

$$I(\tau) = \begin{cases} 0.7089 \left(\tau^{-4}/_{10} + \tau^{-14}/_{315} + \tau^{-24}/_{600} \right) & \tau > 1 \quad (6a) \\ 1 - 1.1046\tau + 1.0141 \left(\tau^{4}/_{6} + \tau^{10}/_{135} + \tau^{16}/_{600} \right) & \tau < 1 \quad (6b) \end{cases}$$

For B2 ordering Inden obtained 7a and 7b by counting the number of different bonds;

$$\Delta H_{T=0}^{dis \rightarrow ord} = \begin{cases} -RX_{Al}^2 \; (4W^1 - 3W^2) & 0 < X_{Al} \leq 0.5 \quad (7a) \\ -R(1-X_{Al})^2 (4W^1 - 3W^2) & 0.5 \leq X_{Al} < 1 \quad (7b) \end{cases}$$

and the Bragg-Williams approximation yields;

$$T_C = X_{Al}(1-X_{Al}) \; (8W^1 - 6W^2) \tag{8}$$

W^1 and W^2 are the so called"exchange energies"(expressed in k-units) for the nearest and next nearest neighbours. The Bragg-Williams approximation does not account for short range order and consequently it predicts a critical temperature T_C which is too high. Inden found that one could introduce a correction factor κ to the value calculated by means of Eq. 8 and obtain good agreement with calculations based on the cluster-variation method which do account for short range order.

3. Application to the Fe-Al Phase Diagram

For Fe-Al Inden (2) reports W^1=1478 and W^2=794 (k-units, k=13.8.10^{-24} J/atom) and κ=0.68. By applying these values it is possible to calculate the critical temperatures for B2 and DO_3 ordering. This was done by Miodownik (8) who also made a comparison with experimental information and

found the calculated temperatures too low. To obtain agreement with the experimental temperatures at X_{Al}=0.25 he chose W^1=1588 but kept the other values unchanged. A further investigation reveals that there are still large discrepancies when $X_{Al}<0.25$ or $X_{Al}>0.25$. To obtain a better agreement over the whole composition range W^1 and W^2 must be allowed to vary with composition. This can be done with a reasonable increase in effort and good agreement with the low-temeprature data is then obtained. However, it is found that this procedure overestimates the stability of the bcc-phase relative to the liquid at high Al-content ($X_{Al}\gtrsim 0.4$) where no information on the critical temperatures is available. To overcome this problem it is necessary also to introduce temperature-dependencies in W^1 and W^2. It is a substantial increase in complexity to evaluate both a concentration and temperature dependency and it was thus decided to accept Miodownik's parameters to avoid these difficulties.

Eqs. 5-10 completely determine the term $G_m-G_m^{dis}$ in Eq. 1. The remaining thermodynamic quantities are now to be determined to comply with the available information.

Kaufman and Nesor (9) analyzed the Fe-Al phase diagram without distinguishing between the ordered and disordered bcc-phase. The present analysis follows their evaluation except that the ordering has been accounted for. The total Gibbs energy of the bcc-phase was obtained by adding the ordering contribution given by Eq. 5 to the Gibbs energy of the disordered solution given by Eq. 2. It was then necessary to adjust all parameters given by Kaufman and Nesor and the new parameters are summarized in Appendix A.

4. Calculated Quantities

The recalculated phase-diagram is shown in Figs. 1-3. Fig. 2 shows a magnified view of the compound equilibria and Figs. 3a and 3b show the equilibria with the fcc-phase. In Figs. 4a and 4b comparisons are made with thermochemical data from Hultgren (10) the calculations according to Kaufman and Nesor (9) and the present analysis. While the agreement between the enthalpy of formation as reported by the different sources is satisfactory, there are larger discrepancies for the excess free energy of Al. However, the experimental scatter was large in the latter quantity and the new values fall within the error limits given by Hultgren.

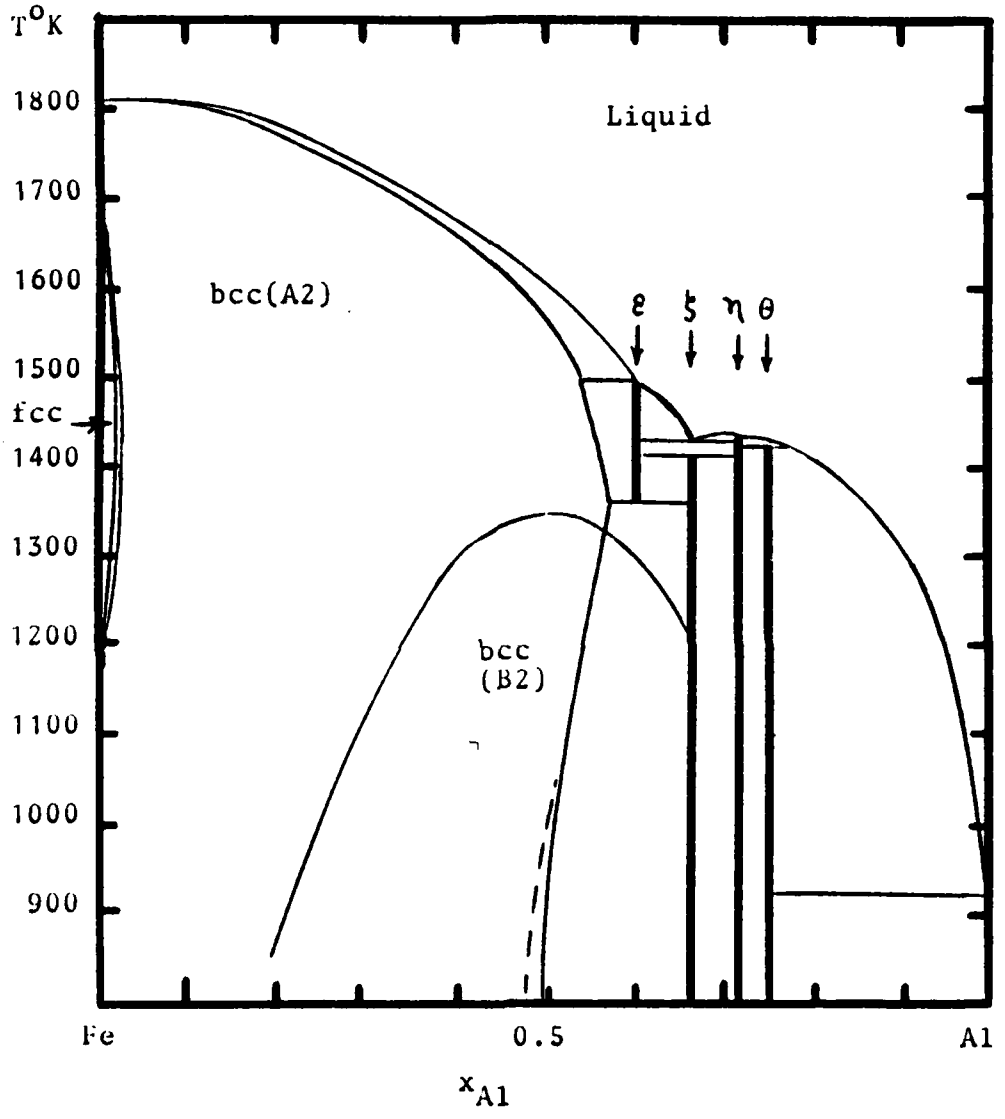

Figure 1. Calculated Iron-Aluminum Phase Diagram (see Figure 3a for the fcc/bcc detailed equilibria)

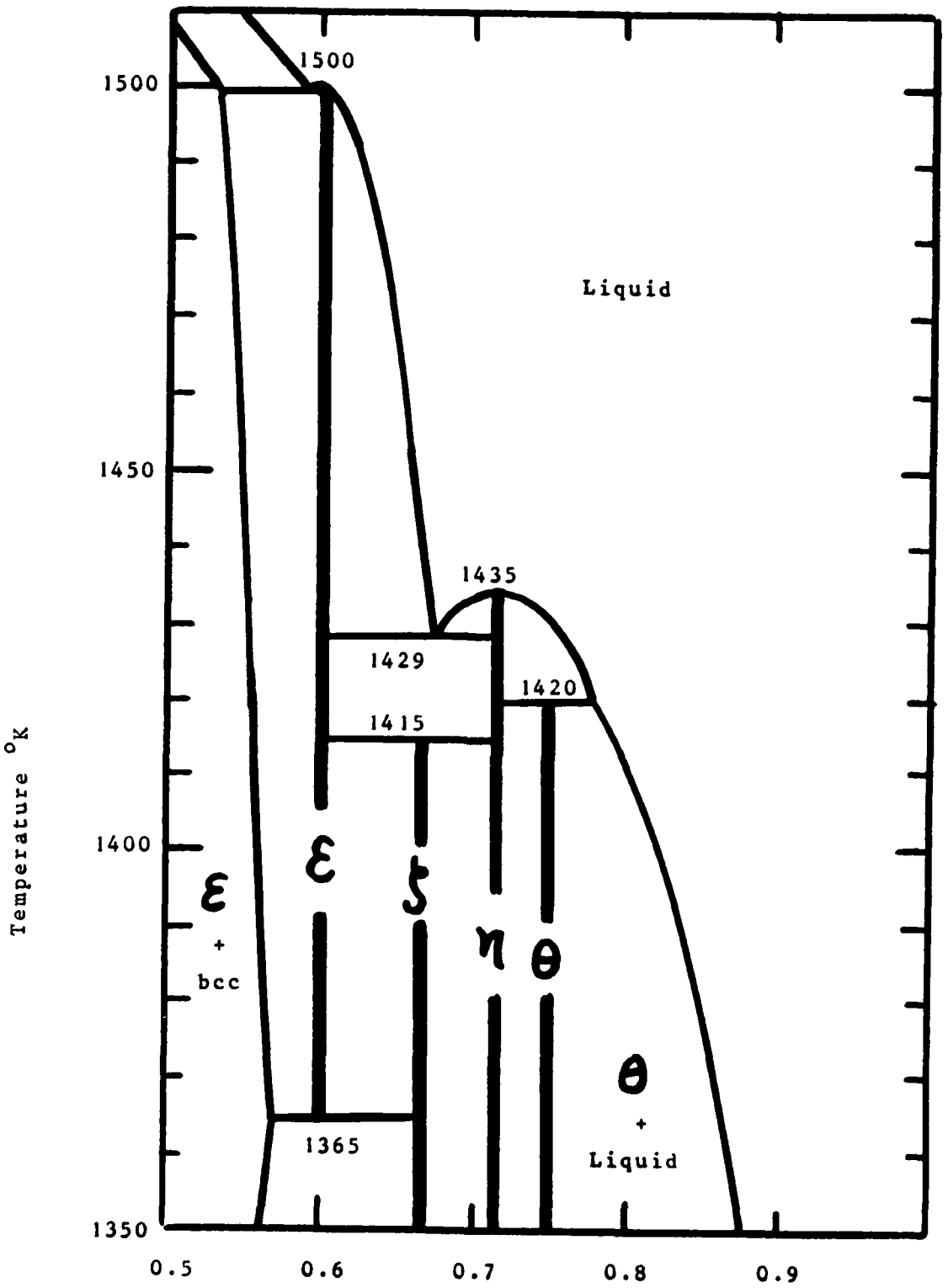

Figure 2. Calculated Compound Equilibria in the Iron-Aluminum System

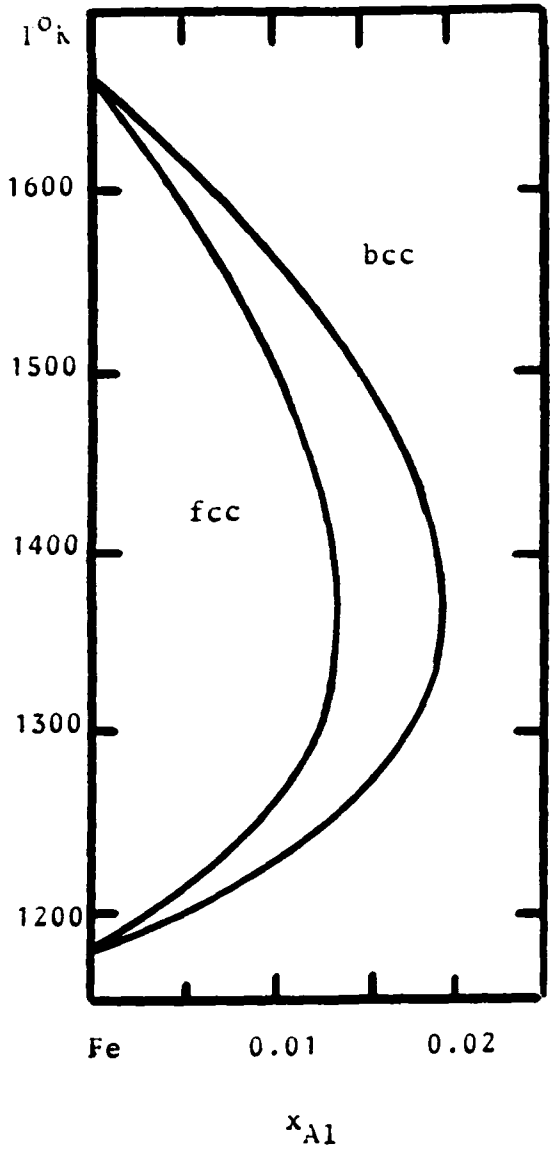

Figure 3a. Calculated bcc/fcc Equilibria in the Iron-Aluminum System.

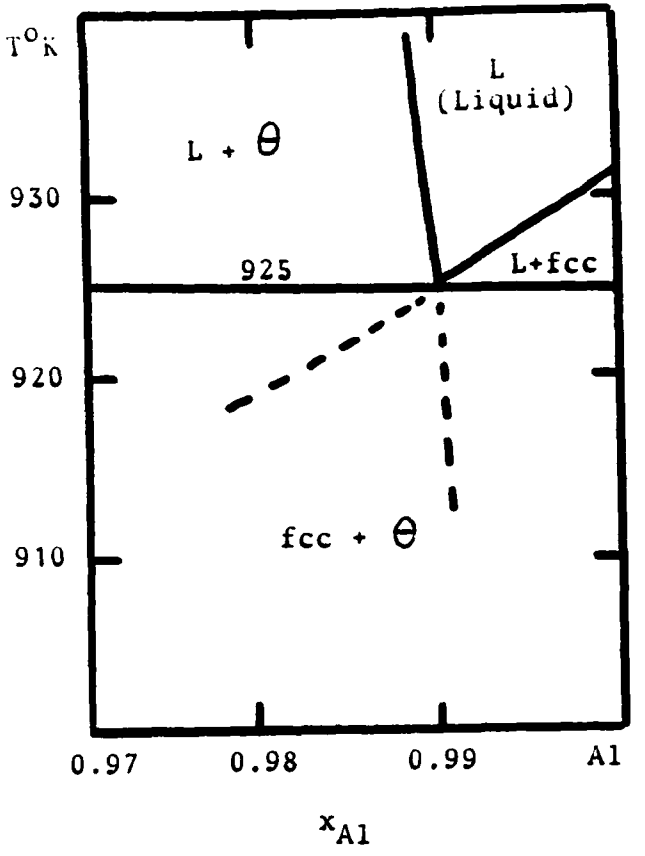

Figure 3b. Calculated Equilibria in the Aluminum-Rich Part of the Iron-Aluminum System.

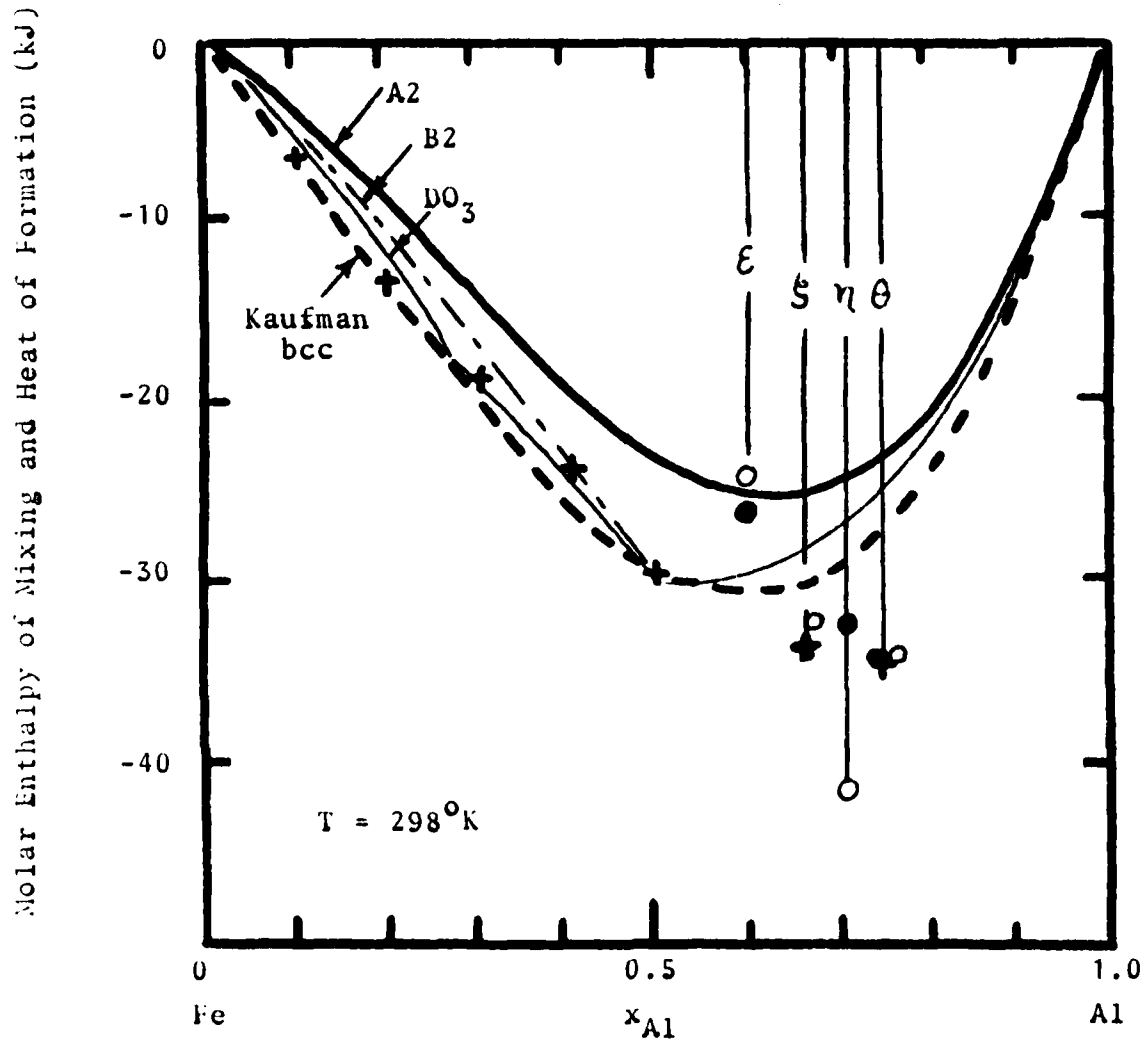

Figure 4a. Molar Enthalpy of Mixing of Iron-Aluminum Alloys and Heat of Formation of Compounds as a function of Composition at 298°K. The Crosses denote the values given by Hultgren (Reference 10), the dashed heavy curve for the bcc phase is due to Kaufman and Nesor (Reference 9) and the open circles for the compound phases is due to Kaufman and Nesor (Reference 9). The remaining curves and the closed circles are from the present analysis.

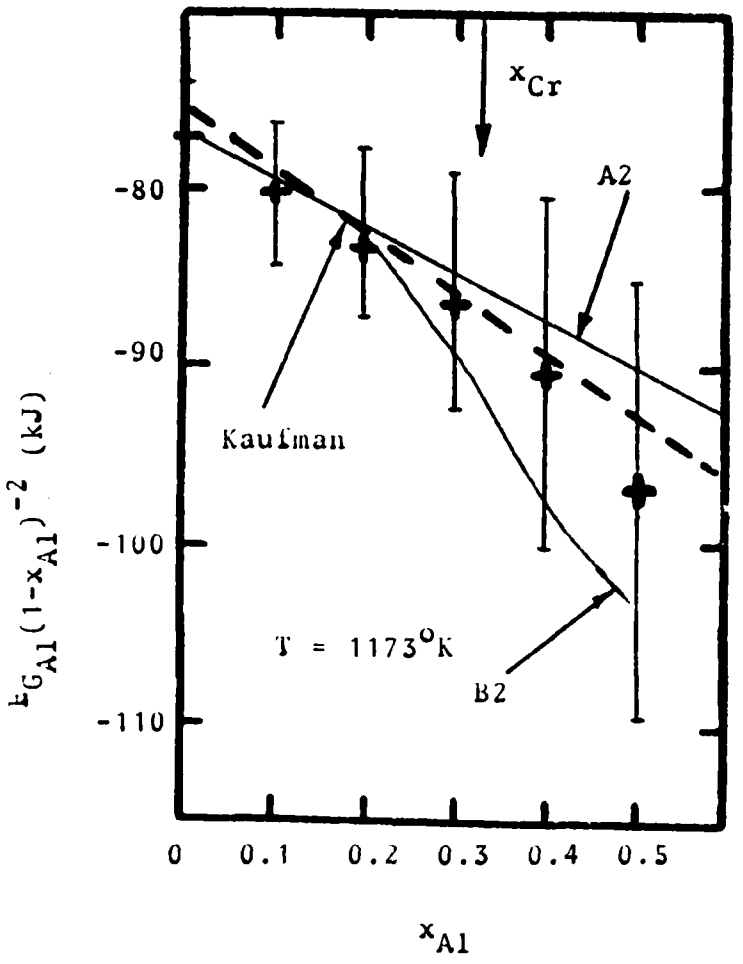

Figure 4b. The Partial Excess Gibbs Free Energy of Aluminum in bcc iron-aluminum alloys at 1173°K divided by the atomic fraction of iron squared shown as a function of the aluminum concentration. The heavy line is due to Kaufman and Nesor (Reference 9) while the crosses (and error bars) are from Hultgren (Reference 10). The remaining curves refer to the present analysis.

5. Subregular Approximation

It is interesting to see to what extent the new formalism can be approximated by a subregular model. The following approximations were obtained for $X_{Al}<0.5$ by plotting the quantity $\Delta G/X_{Al}X_{Fe}$ and fitting a suitable straight line to the resulting curve. The following results were obtained

for $T > T_{cr}$ and $X_{Al}>0.2$

$$\Delta G/X_{Al}X_{Fe} = 2.016.10^{-3}\left(4W^1-3W^2\right)^5 T^{-4}\left(3.75X_{Fe}-11.49X_{Al}\right) \tag{9a}$$

$$X_{Al}<0.2,\ \Delta G = 0 \tag{9b}$$

For $T<T_{cr}$

$$\Delta G/X_{Fe}X_{Al} = R(4W^1-3W^2)\quad\left(0.4444X_{Fe} - 2.4126X_{Al}\right)$$

$$-R\,\frac{1.1046}{2\kappa}\quad T\left(0.9789X_{Fe} - 8.8171X_{Al}\right)$$

$$-T^4/\left(4W^1-3W^2\right)^3\quad\left(68.19X_{Fe} + 142X_{Al}\right)$$

where $\Delta G = {}^{E}G^{bcc} - {}^{E}G^{bcc}_{(dis)}$ (10)

with the actual values for Fe-Al inserted we obtain (with A2=disordered bcc)

$T > T_{cr}$, $X_{Al} > 0.2$:

$$G_m^{ord}-G_m^{A2} = X_{Fe}X_{Al}\left(7.455\ 10^{15}\ X_{Fe} - 22.844\ 10^{15}X_{Al}\right)T^{-4} \tag{11}$$

$T < T_{cr}$:

$$G_m^{ord}-G_m^{A2} = X_{Fe}X_{Al}\left[\left(14669-6.61T-1.09\ 10^{-9}\ T^4\right)X_{Fe}\right.$$
$$\left. +\quad\left(-79635 + 59.54T - 2.27\ 10^{-9}\ T^4\right)X_{Al}\right] \tag{12}$$

Both above and below the critical temperature a strong asymmetric term is obtained. The temperature dependencies T^{-4} and T^{4} are also strong.

In Figs. 5a, b, c and d these approximation formulas have been compared with Eqs. 5-8. The agreement is quite good except in the transition region between disordered and ordered state.

6. Calculation of Isothermal Sections in Fe-Al-X, X=Mn,Ni

Once the thermodynamics of the binary solutions have been established the properties of a ternary phase can be evaluated directly, assuming that there are no specific ternary effects. In a rigorous treatment the order disorder contribution is still given by eqs. 5-6, but ΔH and T_c are now to be evaluated for the actual ternary composition. It is a straight forward procedure to derive expressions for ΔH and T_c in the ternary case but the final expressions are rather complicated. In the present case a simpler approach will be taken. The Kohler method has been applied frequently to synthesize the properties of a ternary solution when the binaries are known, see for example ref.11 . Admittedly there is no physical justification for this method in the present case and its general features have recently been questioned(12). However, the use of the method is widespread and, for the sake of simplicity, it was applied here as follows: First a ternary calculation was made using the subregular model assuming a completely disordered bcc-phase described by the Kohler method. Thereafter a new calculation was performed with the order-disorder contribution added. When $X_{Al}/(X_{Fe}+X_{Al}) < 0.20$ the latter contribution is approximately zero, as can be seen from Fig. 5, and the phase boundaries follow the first set of curves. When $X_{Al}/(X_{Fe}+X_{Al}) > 0.30$ the subregular solution approximation is a good approximation of the order-disorder contribution and the phase boundaries thus follow the second set of curves. The curves in the transition region were drawn by hand assuming a gradual shift from one set of curves to the other set.

All parameters, except those for Al-Fe, were taken from the ManLabs data bank (14). The results are presented in Figs. 6-7

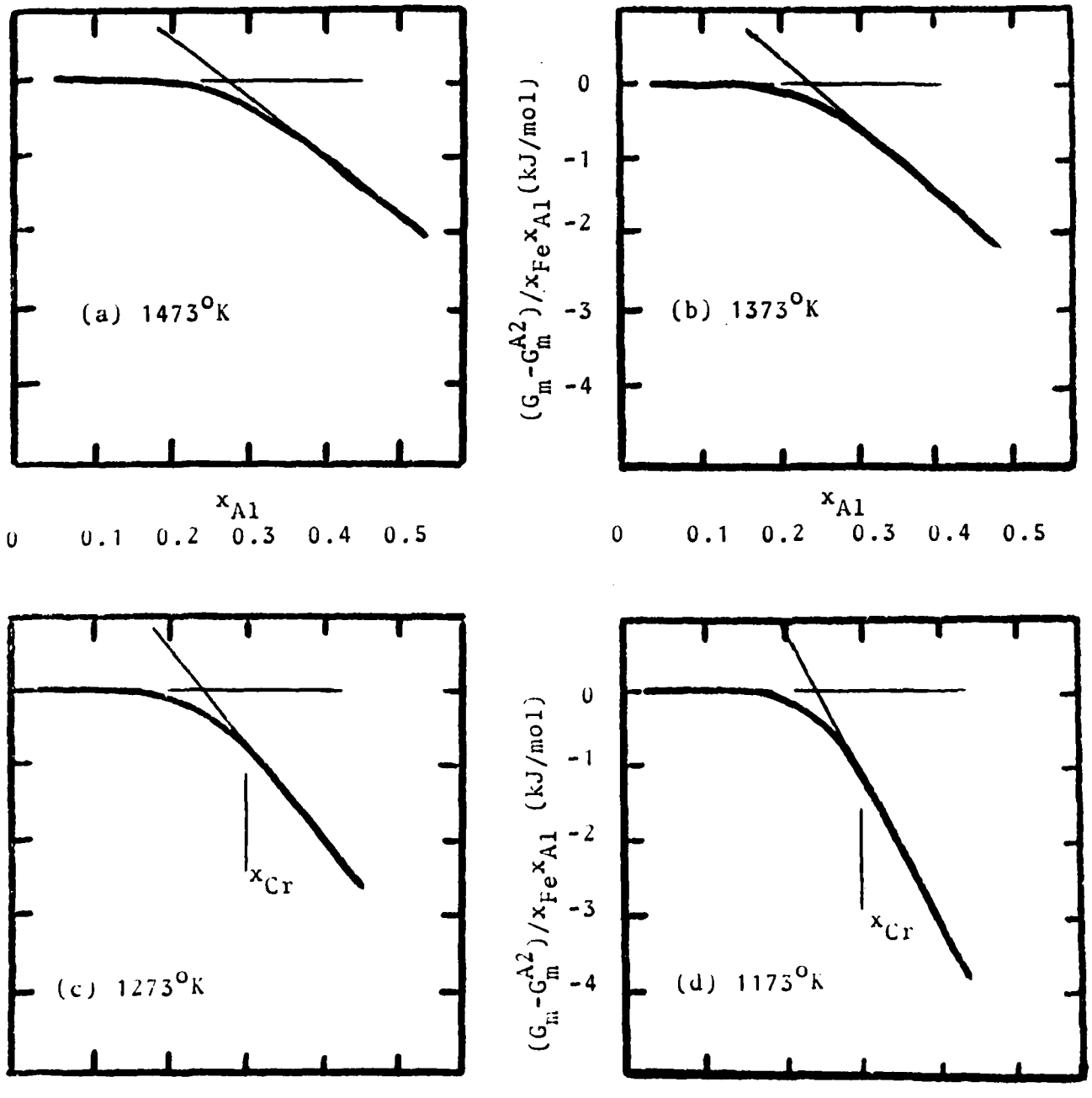

Figure 5. Calculated regular solution parameter for bcc Iron-Aluminum alloys as a function of composition at various temperatures. The thick curve represents the present analysis while the thin segments represent the subregular approximation.

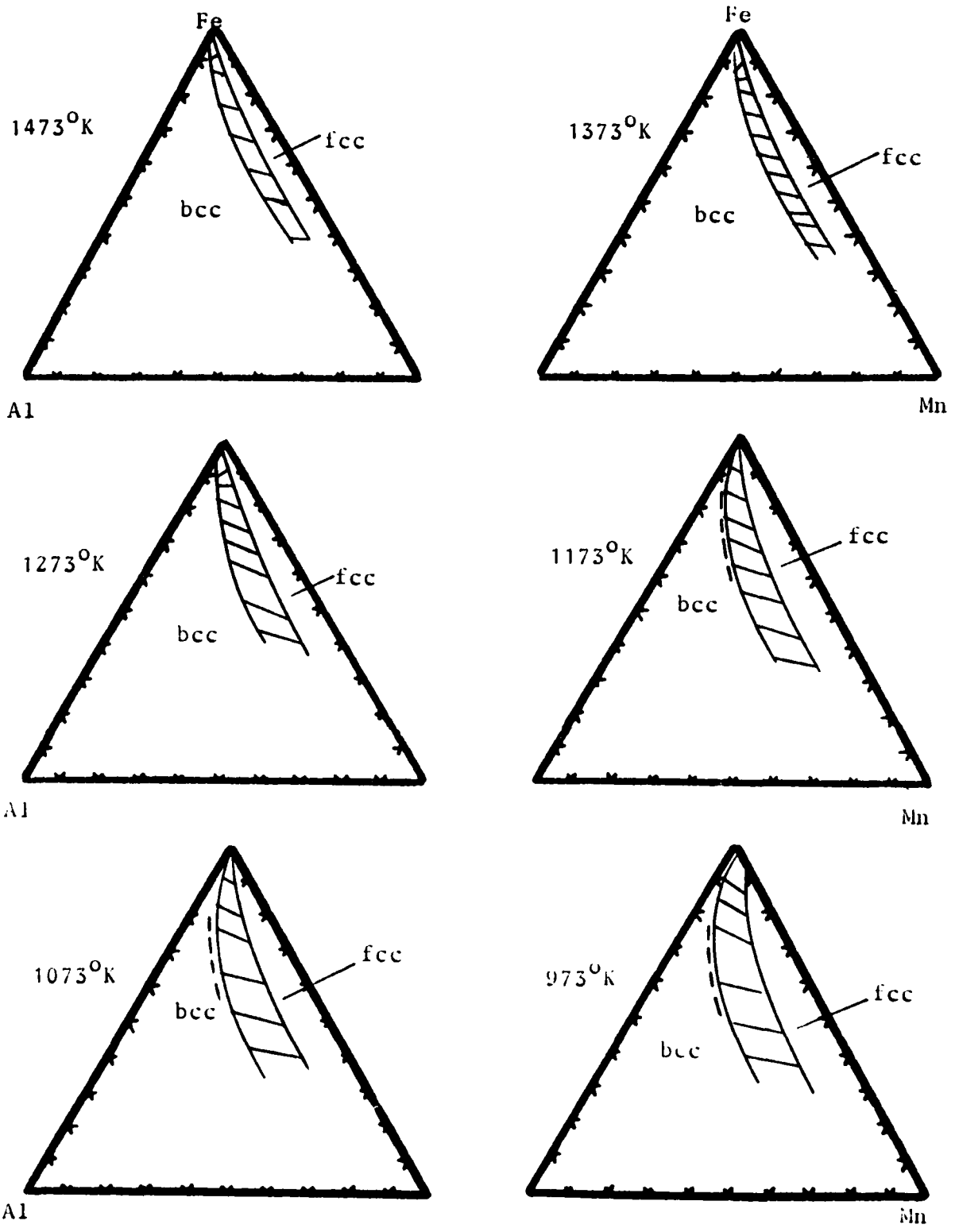

Figure 6. Calculated fcc/bcc Equilibria in the Iron-Manganese Aluminum System as a function of temperature between ordered bcc and fcc solid solutions. The dashed curve shows the phase boundary for the disordered bcc phase. No difference was noted above 1173°K.

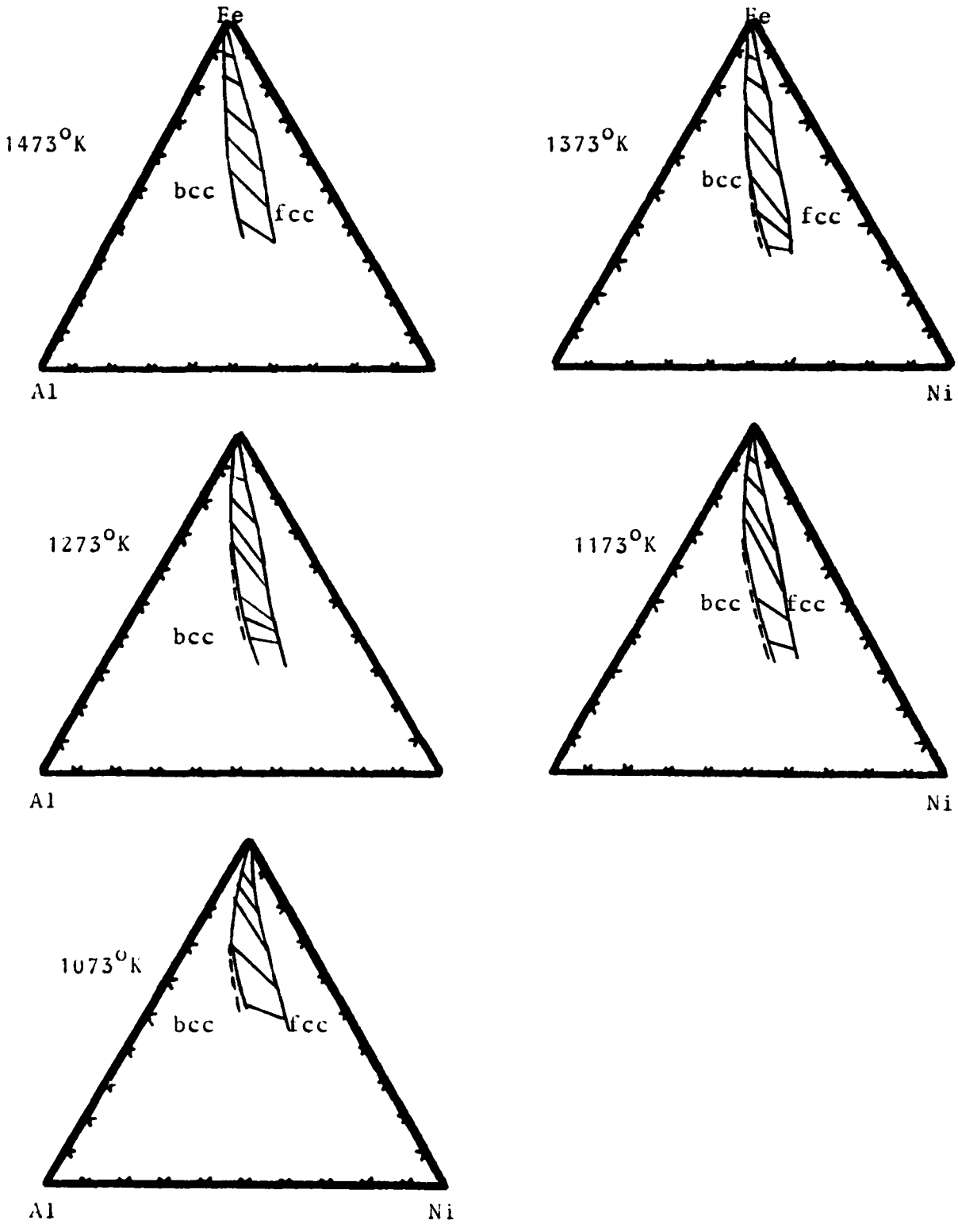

Figure 7. Calculated fcc/bcc Equilibria in the Iron-Nickel-Aluminum System as a function of temperature between ordered bcc and fcc solid solutions. The dashed curve shows the phase boundary for the disordered phase.

It can be seen that the order-disorder contribution to the Gibbs energy generally yields a very small shift of the calculated phase boundaries. Furthermore, a comparison with the calculations by Kaufman, (13) who did not distinguish between ordered and disordered state, shows that there are no significant discrepancies. The curves fall very close to each other.

It will now be argued that the present procedure probably overestimates the effect of ordering on the bcc/fcc equilibrium. For a given temperature the composition range within which ordering occurs is approximately given by the parabola: $X_{Al}\ X_{Fe}$ = constant which starts from the binary Al-Fe-side and loops into the ternary. The exact relation is complicated (8) and requires detailed knowledge about the order-disordering reactions in the other two binaries. The parabola is a reasonable approximation when the maximum ordering temperatures are low (but still above $0^{o}K$) in the other systems. In Fig. 8 the parabola has been plotted at different $X_{Al}\ X_{Fe}$ values. When these plots are superimposed on the calculated bcc/fcc equilibria it is found that all temperatures the bcc/fcc phase boundary falls well outside the field of ordered bcc. It is thus concluded that the true phase boundaries must follow the ones calculated with a disordered bcc phase.

As a final conclusion, it would be worthwhile to examine the degree of order at each composition in the bcc phase at the two phase bcc + fcc boundary. For consistency this degree of order should coincide with the degree of order in the iron-aluminum binary at the same X_{Al}/X_{Fe} ratio which characterizes the ternary composition. If this is <u>not the case</u>, then the ternary free energy synthesized from the binary components incorrectly reflects the wrong degree of order. In the present case the errors introduced by such an inconsistency do not appear to be very large. However, it is possible that such errors could be substantial in other cases and should be guarded against.

Note in Proof

The prior discussion of Section 3 drew attention to the discrepancy between the experimental ordering temperature and the calculated value for $0.25 \leq X_{Al} \leq 0.50$. It was noted that compositionally dependent values of

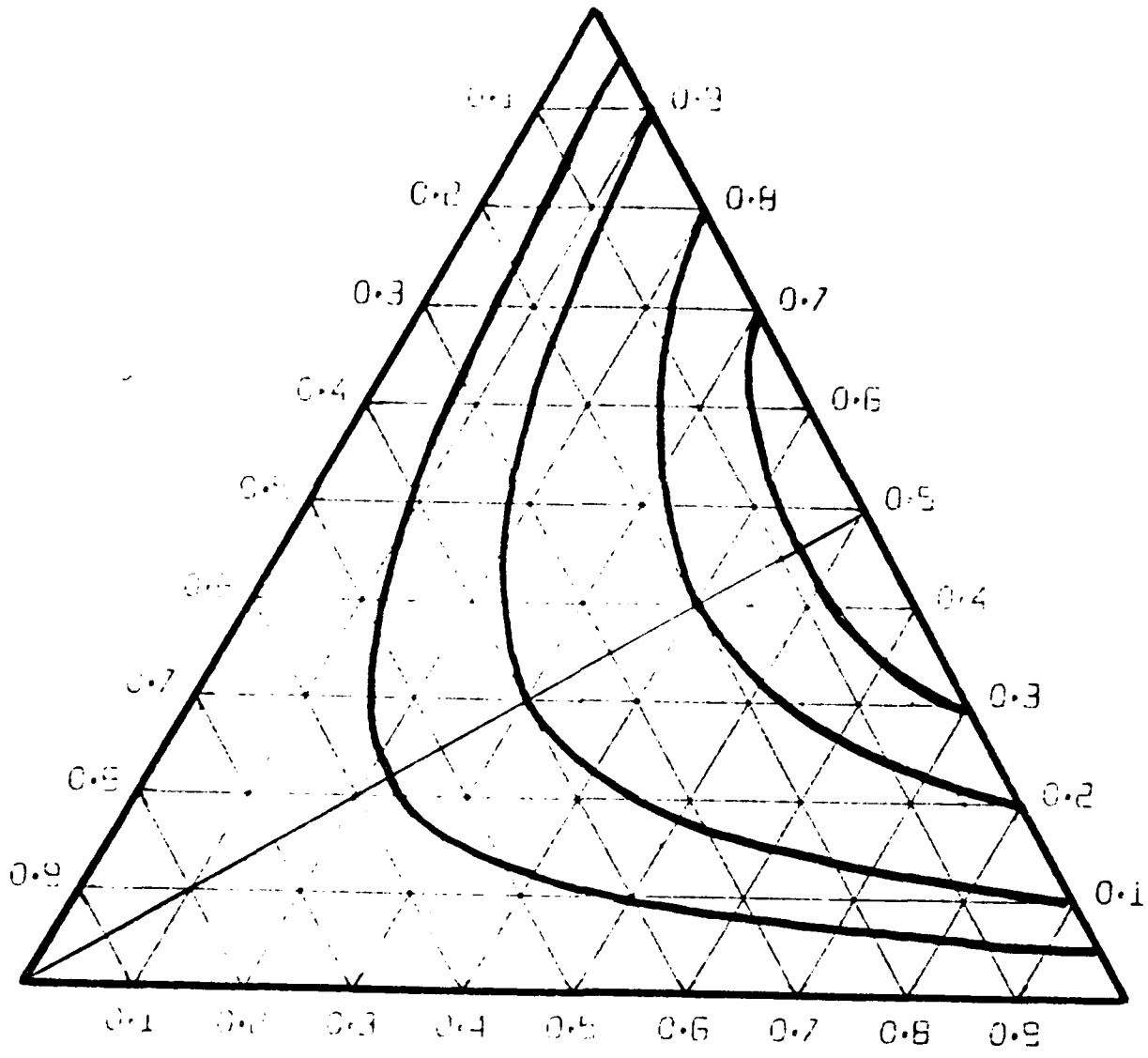

Figure 8. Parabola $X_A X_B$ = constant at different values of the constant.

W^1 and W^2 would be required to eliminate this discrepancy. It was also noted that such an alteration would lead to a stabilization of the bcc phase at high temperature and a resulting excessive elevation of the melting points. Notwithstanding these difficulties an attempt was made to evaluate W^1 and W^2 as a function of composition in order to produce an ordering temperature vs. composition curve for $0.25 \leq X_{Al} \leq 0.50$ (8) corresponding to 1260K at X_{Al} = 0.30 and 1570K at X_{Al}= 0.40. The resulting expression for W^1 is given by Equations 13 and 14 as:

$$W^1 = 1480 + 625\ X_{Al} \qquad (13)$$

and

$$W^2 = 846 - 372\ X_{Al} \qquad (14)$$

These new values compare with the previous values of W^1 = 1478 and W^2 = 794 listed in Section 3. These expressions for W^1 and W^2 as provided by Equations (13) and (14) were substituted directly into Equations (5) through (8) to reformulate the thermochemical properties of the iron-aluminum system. No further changes in the remaining parameters for the iron-aluminum system were made at this stage. This procedure did indeed produce an excessive stabilization of the bcc phase with respect to the liquid. Nevertheless, this new formulation of the bcc phase was employed directly to derive an effective subregular description as in Section 5. The latter step was accomplished by evaluating W^1 and W^2 at X_{Al} = 0.5 from Equation 13 and 14 since at X_{Al} = 0.5 the largest difference between this approximation and the former calculation exists. Thus for this case W^1 = 1793 and W^2 = 660. Employing these values in Equations (9) and (10) permits redefinition of the excess free energy of iron-aluminum alloys in the subregular approximation. Subsequent recalculation of the Fe-Ni-Al fcc/bcc equilibrium at 1273 with the modified results did not yield results significantly different from those shown in 7c. It is therefore concluded that the results described in Section 6 would not be materially altered by introducing compositionally dependent values of W^1 and W^2 for the purpose of obtaining a better description of the ordering temperature at compositions containing more than 25 atoms percent aluminum.

References

1. G. Inden: Acta Met. 22 (1974) p 945.

2. G. Inden: Project Meeting CALPHAD V 21-25 June 1976, Max-Planck-Institut fur Eisenforschung G.m.b. H, Dusseldorf/W. Germany, p 4-1.

3. G. Inden: Ibid, p 111. 4-1.

4. S. Hertzman and B. Sundman: CALPHAD (in print)

5. M. Hillert and M. Jarl: CALPHAD, 2 (1978) p 227.

6. J. Agren: Met Trans A, 10A (1979) p 1847.

7. G. Inden: personal communication

8. A.P. Miodownik: Computer Based Methods for Thermodynamic Analysis of Materials Processing, ManLabs, Inc., Cambridge, Mass. 02139 November 1981, Contract F49620-80-C-0020 AFOSR Bolling AFB (D.C. 20332).

9. L. Kaufman and H. Nesor, CALPHAD 2 (1978) p 325.

10. R. Hultgren et. al.: Selected Values of the Thermodynamic Properties of Metals (and Binary Alloys), (2 volumes) ASM, Metals Park, Ohio (1973).

11. L. Kaufman: CALPHAD, 1 (1977) p.7

12. J. Brynestad: CALPHAD, 5 (1981) p. 103

13. L. Kaufman (in ref. 8)

14. ManLabs-NPL, Materials Data Bank, Instruction Manual, ManLabs, Inc. Cambridge, Mass. 02139

Appendix A: Summary of Parameters for the Fe-Al System

The lattice stabilities from Ref. 9.

$$^{E}G_{m}^{bcc,dis} = X_{Fe}X_{Al}\,(-32345-37.92T)X_{Fe} + (-150252+51.42T)X_{Al} \quad \text{J/mol}$$

$W^1 = 1588$, $W^2 = 794$ (k units $k=13.8\cdot10^{-24}$ J/atom), $K=0.68$

$$^{E}G_{m}^{fcc} = X_{Fe}X_{Al}\,(-25022-38.01T)X_{Fe} + (-106841+66.70T)X_{Al} \quad \text{J/mol}$$

$$^{E}G_{m}^{L} = X_{Fe}X_{Al}\,(-62760-14.63T)X_{Fe} + (-96232+32.72T)X_{Al} \quad \text{J/mol}$$

$$^{\circ}G^{\theta}_{Fe_{0.25}Al_{0.75}} - 0.25\,^{\circ}G_{Fe}^{bcc} - 0.75\,^{\circ}G_{Al}^{bcc} = -35275+8.28T \quad \text{J/mol}$$

$$^{\circ}G^{\eta}_{Fe_{0.286}Al_{0.714}} - 0.286\,^{\circ}G_{Fe}^{bcc} - 0.714\,^{\circ}G_{Al}^{bcc} = -41169+11.40T \quad \text{J/mol}$$

$$^{\circ}G^{\zeta}_{Fe_{0.333}Al_{0.667}} - 0.333\,^{\circ}G_{Fe}^{bcc} - 0.667\,^{\circ}G_{Al}^{bcc} = -37872+4.73T \quad \text{J/mol}$$

$$^{\circ}G^{\varepsilon}_{Fe_{0.40}Al_{0.60}} - 0.4\,^{\circ}G_{Al}^{bcc} - 0.6\,^{\circ}G_{Fe}^{bcc} = -23863-2.77T \quad \text{J/mol}$$

VI A THERMODYNAMIC EVALUATION OF THE TITANIUM-CARBON-NITROGEN PHASE DIAGRAM.

John Agren

1.0 Introduction

The use of vapor deposited TiC, TiN and Ti(C,N) coatings for improving the performance of cutting tools and wear resistant surfaces enhances the value of information on the thermochemistry and phase diagram of the Ti-C-N system.

Since the crystal structures of the compounds TiC and TiN are the same, it is likely that these compounds form a solid solution. However, the experimental Ti-C and Ti-N phase diagrams reported to date are not very well established and very little thermodynamic data is available for the binary cases or the Ti-C-N ternary. The purpose of the present work is to evaluate all the information available in terms of thermodynamic models for the individual phases and synthesize the binary and ternary phase diagrams.

2.0 Thermodynamic Models

2.1 Liquid

The simplest models that cover the whole concentration range are the regular or subregular solution models. The formation of the solid compounds TiC and TiN in the binaries suggests that some ordering or formation of molecular species might take place in the liquid around the stoichiometric compositions. However, a high degree of association is not observed in the gas phase and vaporization of titanium carbide yields titanium and carbon polymers. The Fe-S system has recently been treated by assuming the presence of molecular species (1) and by assuming ordering (2). Both treatments yield a satisfactory agreement with experimental data, and predict a very rapid change in activity close to the stoichiometric composition. This rapid change is difficult to describe with a regular or subregular solution model, and generally many terms will be needed in the series expansion of the excess energy.

The abnormal behavior of the activity, compared to what the regular solution model predicts, reveals itself in the phase-diagram by giving the compound a liquidus curve formed more like a wedge instead of a parabola.

In the present case the experimental data on the L/TiC (liquid/TiC) and L/TiN equilibia is too meager to reveal the shape of the liquidus curves accurately, and no thermodynamic data for the liquid phase is available. For the sake of simplicity the liquid was thus described with the subregular solution model. The corresponding equations are summarized in Appendix B.

2.2 Solid Phases

The TiC and TiN phases both have a Nacl-structure. However, a rather wide range of homogenuity is observed: $Ti_{(1-x)}C_x$ with $0.32 < x < 0.49$. First an attempt was made to describe TiC as a subregular solution. This attempt was not very successful and a new approach was tried. From the crystallographic point of view TiC and TiN consists of two sublattices and the variation in composition is due to a varying number of vacant carbon or nitrogen sites. (3). It was thus decided to apply the sublattice model which was developed by Hillert and Staffansson (4) and later generelized by Sundman and Agren (5) and recently applied to the Fe-S system (2). This approach was more successful and yielded a satisfactory description of all the available information.

Hexagonal titanium exhibits a rather large solubility for N and the choice of thermodynamic model might be important. Recently (6) the hexagonal solution of N in Fe was treated by means of the sublattice model. In agreement with that treatment we chose the upper limit of N-solubility in hcp-Ti as 1/3 corresponding to the compound Ti_2N. For the bcc-phase we also applied the sublattice model with 3 interstials per Ti-atom as in the Fe-C-case (see Ref.6)

The equations for the sublattice model are summarized in Appendix B.

3.0 Evaluation of Parameters for Phases in the Titanium-Carbon System

The free energy of formation of stoichiometric TiC has been tabulated by Hultgren (3). Figure 1 shows the data given by Hultgren as symbos and the solid line is a least square fit (assuming a linear temperature dependency) to the data. The dashed line is calculated according to the parameters given by Kubaschewski and Alcock (7). The result of the least square fit is:

$$ {}^{o}G^{fcc}_{TiC} - {}^{o}G^{bcc}_{Ti} - {}^{o}G^{Gr}_{C} = -45012 + 3.428T \quad \text{(cal/mol)} \quad (1) $$

and was accepted in the present study. Storms (8) has compiled data on the Ti partial pressure over TiC at equilibrium with graphite at different temperatures (See Fig. 2) Kubaschewski and Alcock (7) give the vapor-pressure of pure Ti as:

$$ \log P^{o}_{Ti} = -24400/T - 0.91 \log T + 10.299 \quad (2) $$

From Eq2 we can evaluate the corresponding free energy difference;

$$ {}^{o}G^{gas,\ 1atm}_{Ti} - {}^{o}G^{bcc}_{Ti} = 111645 - 47.124T + 1.808\ T\ln T \quad \text{(cal/mol)} \quad (3) $$

By combining the information from Storms (8) with Eq.3 and

$$ {}^{o}G^{fcc}_{Ti} - {}^{o}G^{bcc}_{Ti} = -240 + 0.9T \quad \text{(cal/mol)} \quad (4). $$

from Kaufman (9) and take the composition of TiC in equilibrium with graphite as $x^{fcc}_{C} = 0.49$ according to Rudy's phase diagram (10) we can calculate the partial excess quantities ${}^{E}G_{Ti}$ and ${}^{E}G_{C}$ as functions of temperature for this particular composition. The phase-boundary Ti/TiC, as reported by Rudy (10), can be used to evaluate ${}^{E}G_{Ti}$ at different temperatures along the phase-boundary when the solubility of C in Ti is neglected. Assuming linear temperature-dependency it was then possible to evaluate ${}^{o}L^{Tifcc}_{CVa}$ and ${}^{1}L^{Tifcc}_{CVa}$ from the partial quantities. The following expressions were obtained:

$$ {}^{o}L^{Tifcc}_{CVa} = -16099 + 0.36T \quad \text{(cal/mol)} \quad (5a) $$

$$ {}^{1}L^{Tifcc}_{CVa} = -38801 + 11.03T \quad \text{(cal/mol)} \quad (5b) $$

The solid line in Figure 2 is calculated by the application of Eqs. 5a and 5b. The agreement with the experimental information is

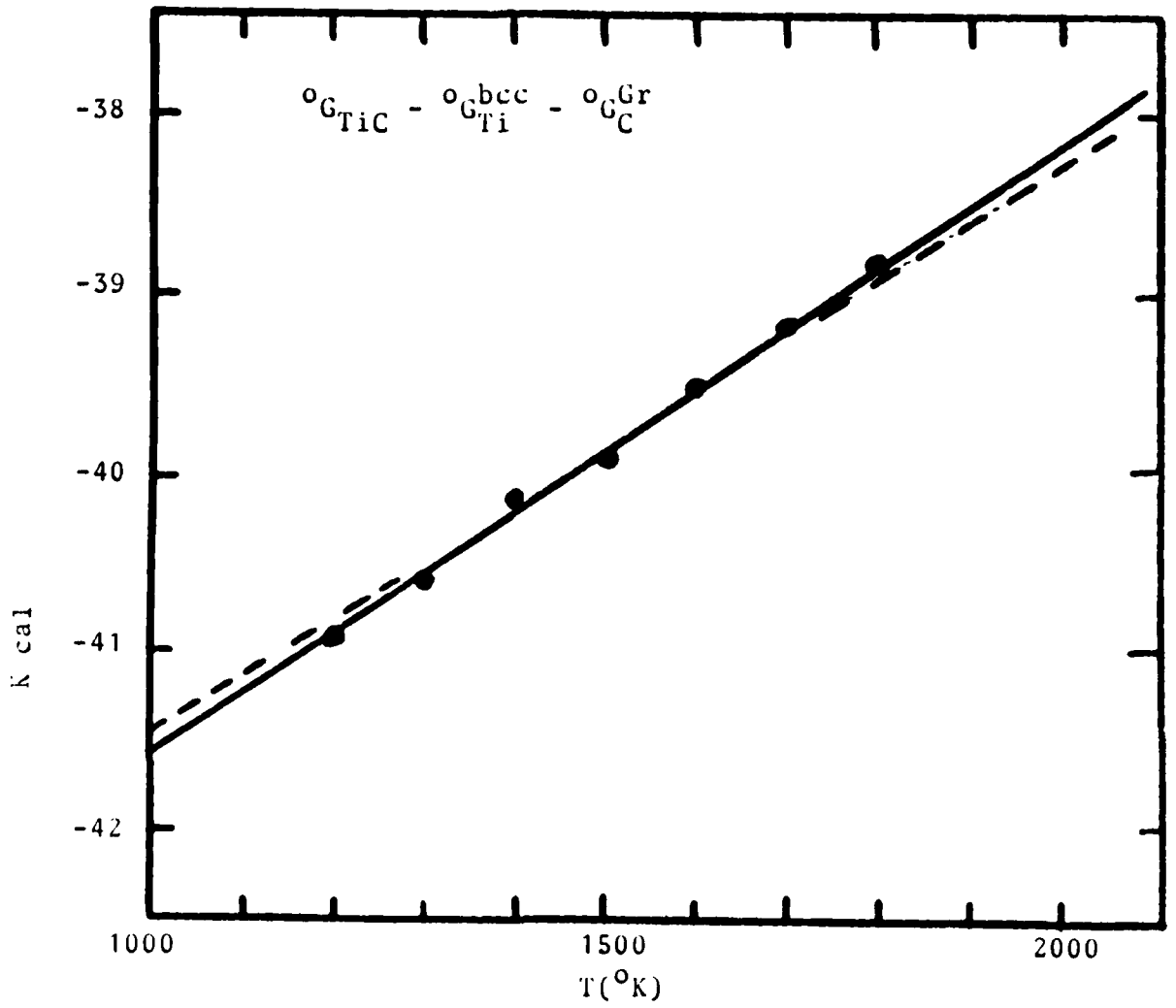

Figure 1. The Free Energy of Formation of TiC from bcc Ti and Graphite as a function of Temperature. Solid Curve designates the present analysis while the Dashed Curve is after Kubaschewski and Alcock (Ref. 6) and the points are from Hultgren (Ref. 3)

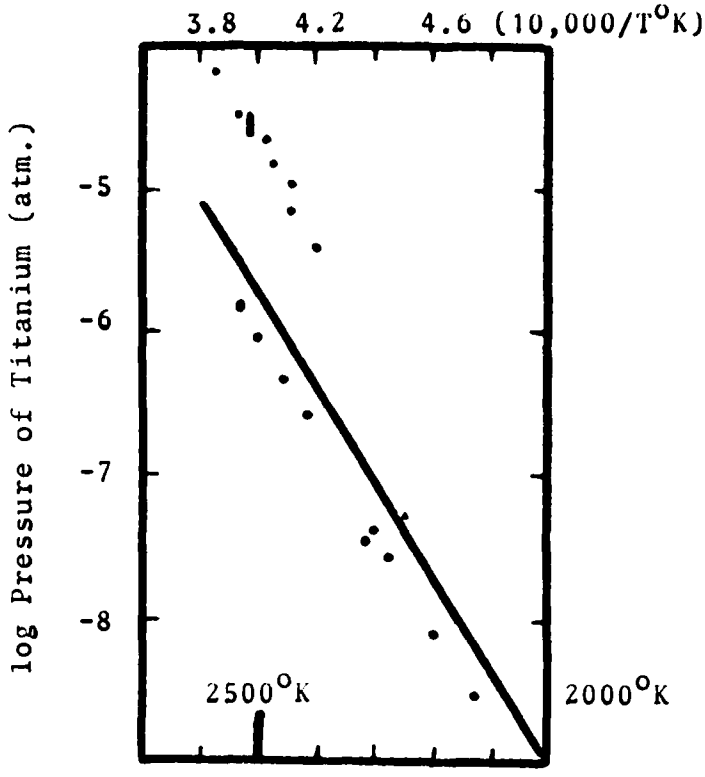

Figure 2. Pressure of Titanium over TiC + Graphite as a function of Temperature. Solid curve is from the present analysis, points are from Ref. 7.

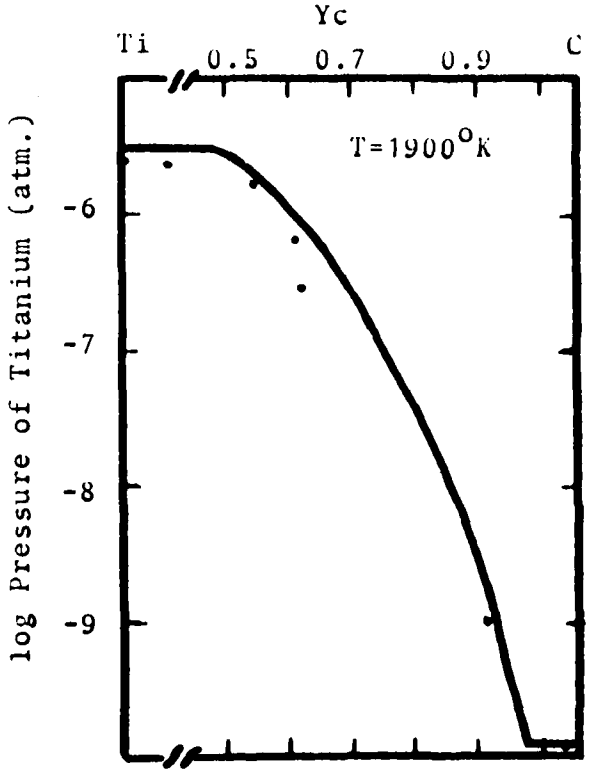

Figure 3. Pressure of Titanium over TiC at 1900°K. Solid Curve is from Present Analysis. Points are from Ref.7.

very good. In Figure 3 the Ti partial pressure as a function of composition at 1900 K has been plotted. The symbols are experiments reported by Storms (8) and the solid line is calculated from the present analysis. The agreement is satisfactory.

The position of the melting-point of TiC according to Rudy (10) is $x_C = 0.44$ and $T_m = 3340$k. By applying the new evaluation of TiC and the lattice stabilities reported by Kaufman (9) one can evaluate the subregular solution parameters that yield this melting-point. Furthermore, temperature dependencies in these parameters can be evaluated from the condition that the L/TiC/Gr eutectic occurs at 3049K and the L/TiC/Ti eutectic at 1923K (from Ref. 10.) The following values are then obtained:

$$ {}^{o}L^{L}_{CTi} = -23185 - 10.5T \quad \text{(cal/mol)} \quad (6a) $$

$$ {}^{1}L^{L}_{CTi} = 30516 - 10.5T \quad \text{-11-} \quad (6b) $$

The sublattice model for the bcc-phase yields a reasonable description with the following parameters:

$$ L^{Tibcc}_{CVa} = -50000 \quad \text{(cal/mol)} \quad (7a) $$

$$ {}^{o}G^{bcc}_{TiC_3} - {}^{o}G^{hcp}_{Ti} - 3\,{}^{o}G^{gr}_{C} = -44996 + 0.49T \quad (7b) $$

The hcp-phase has a very low solubility of carbon and it is thus difficult to evaluate the interaction parameter. Arbitrarily, this was chosen the same as in bcc i.e.

$$ L^{hcp}_{CVa} = L^{bcc}_{CVa} = -50000 \quad \text{(cal/mol)} \quad (8a) $$

Subsequently

$$ {}^{o}G^{hcp}_{Ti_2N} - 2\,{}^{o}G^{hcp}_{Ti} - 1/2\,{}^{o}G^{Gr}_{C} = 5574 \quad (8b) $$

was chosen to yield a three-phase equilibrium fcc/bcc/hcp at 1193K.

All parameters are summarized in Appendix B.

4. Evaluation of Parameters for Phases in the Titanium-Nitrogen System.

In general the data for the TiN-System is meager. The phase diagram given by Hultgren (3) is not very well established and is basically the same as the one in Hansen's compiliation (11).

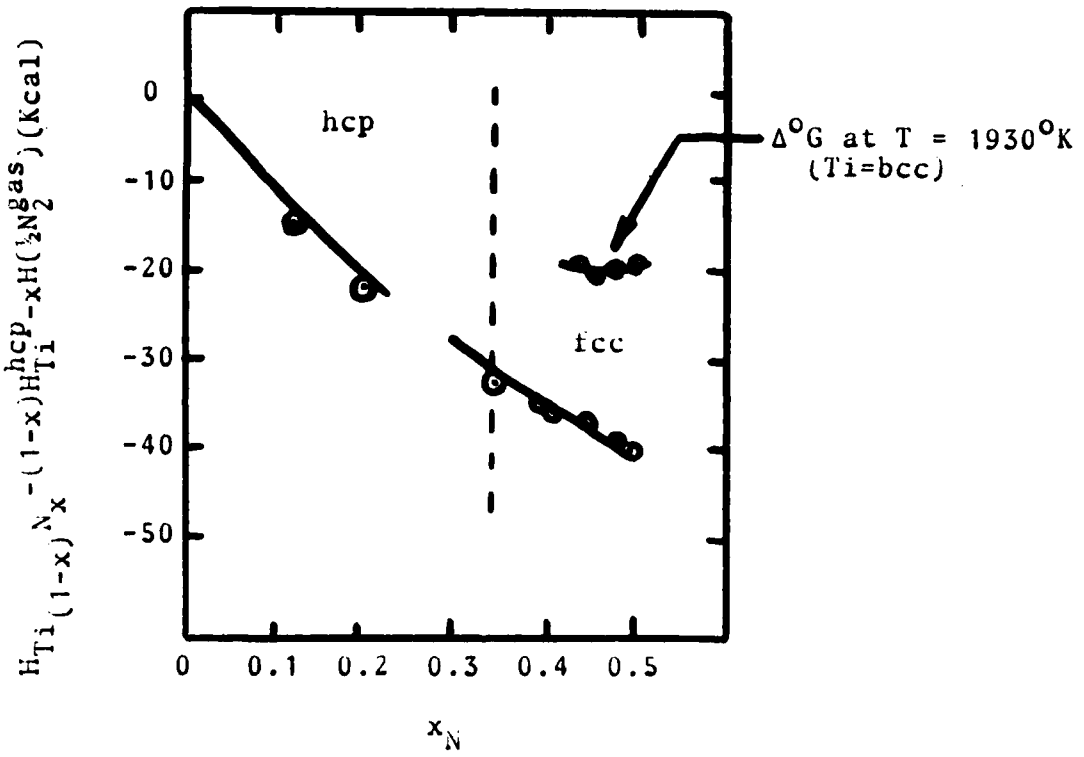

Figure 4. Enthalpy and Gibbs energy change for the reaction
$(1-x)Ti(hcp)+x(\frac{1}{2}N_2 gas,\ 1\ atm.) \rightarrow Ti_{(1-x)}N_x$

Solid curves calculated: Symbols after Hultgren Reference 4.

The free energy of formation for stoichiometric TiN however, seems well known. A least square fit to the values given by Hultgren (3) yields:

$$ {}^{o}G^{fcc}_{TiN} - {}^{o}G^{hcp}_{Ti} - 1/2\ {}^{o}G^{gas}_{N_2} = -79666 + 21.42T \qquad \text{(cal/mol)} \quad (9) $$

This expression yields values in good agreement with those calculated for Kubaschewski and Alcock (7). In addition some information on the enthalpy of mixing in the solid phases is available from Hultgren. Hultgren also gives the free energy of mixing for $0.45 < x_N 0.5$ at 1930K. A solution parameter $L^{Tifcc}_{NVa} = -25000 + 4.4T$ was found to describe the information on the fcc phase satisfactory. In Fig. 4 the calculated values have been plotted together with Hultgren's values. The parameters for the hcp-phase was subsequently evaluated from the fcc/hcp phase boundaries as reported by Hultgren. The following values were obtained:

$$ {}^{o}G^{hcp}_{Ti_2N} - 2\ {}^{o}G^{hcp}_{Ti} - 1/2\ {}^{o}G^{gas}_{N_2} = -93490 + 24.71T \qquad (10a) $$

$$ L^{Tihcp}_{NVa} = -9985 - 3.44T \qquad (10b) $$

The enthalpy of mixing in the hcp phase can now be calculated as a function of composition and the result is presented in Fig. 6 together with two experimental values given by Hultgren. The agreement is satisfactory.

In Hultgren's phase diagram a tetragonal phase Ti_2N with a very narrow composition range is shown at low temperatures. This phase was treated as a stoichiometric compound in the present evaluation and it's free energy of formation was evaluated from the reported phase boundary with hcp at 1310K and 1200K, yielding the following expression:

$$ {}^{o}G^{tetragonal}_{Ti_2N} - 2\ {}^{o}G^{hcp}_{Ti} - 1/2\ {}^{o}G^{gas}_{N_2} = -120692 + 43.06T \qquad \text{(cal/mol)} \quad (11) $$

The highest temperature where this phase is stable is then calculated as 1321K.

It is very difficult to evaluate two parameters for the bcc-phase because the N-solubility is rather low. Quite arbitarily it was then chosen to put:

$$ L^{Tibcc}_{NVa} = 0 \qquad (12) $$

The remaining parameter was then adjusted to yield a hcp/bcc equilibrium in reasonable agreement with Hultgren's phase diagram.

The following value was obtained:

$$ {}^{o}G^{bcc}_{TiN_3} - {}^{o}G^{hcp}_{Ti} - 3/2\ {}^{o}G^{gas}_{N_2} = -104155 + 31.22T \qquad (13) $$

No thermodynamic data for the liquid phase is available. The two subregular solution parameters were adjusted to yield an fcc/L equilibrium in reasonable agreement with Hultgrens phase diagram. The following parameters were found:

$$ {}^{o}L^{L}_{NTi} = -64482 - 7.5T \qquad \text{(cal/mol)} \quad (14a) $$

$$ {}^{1}L^{L}_{NTi} = -40975 + 7.5T \qquad \text{(cal/mol)} \quad (14b) $$

All parameters are now fixed and a complete phase diagram can be calculated. The parameters are summarized in Appendix B.

5.0 Calculation of Ti-C Phase Diagram

Combination of the equations in Appendix B and the parameters in Appendix C permit calculation of the phase diagram by standard methods. The result is presented in Fig 5.

Figure 6 compares the experimental points, the phase boundaries (dashed curve) suggested by Rudy (10) and the calculated results (solid lines). The agreement with the suggested solidus curve is very good whereas the agreement with the suggested liquidus curve is not so good. However, the liquidus curve has not been established experimentally to date. It should however, be mentioned that the appearence of order or molecular species in the melt will deform the liquidus curve to a shape more like the one proposed by Rudy. (10).

6.0 Calculation of the Ti-N Phase Diagram

The calculated titanium-nitrogen phase diagram is shown in Fig 7. In addition Hultgrens phase diagram is displayed using dashed lines. The solid-phase equilibria are in a very good agreement and the fcc/L-equilibrium is satisfactory. In both Hansen's and Hultgren's phase diagrams, the latter equilibria was designated by dashed lines to indicate that the shape of the curves is very uncertain. The most serious discrepancy between the reported phase diagram and the calculated one is the temperature of the three-phase equilibrium L/bcc/hcp.

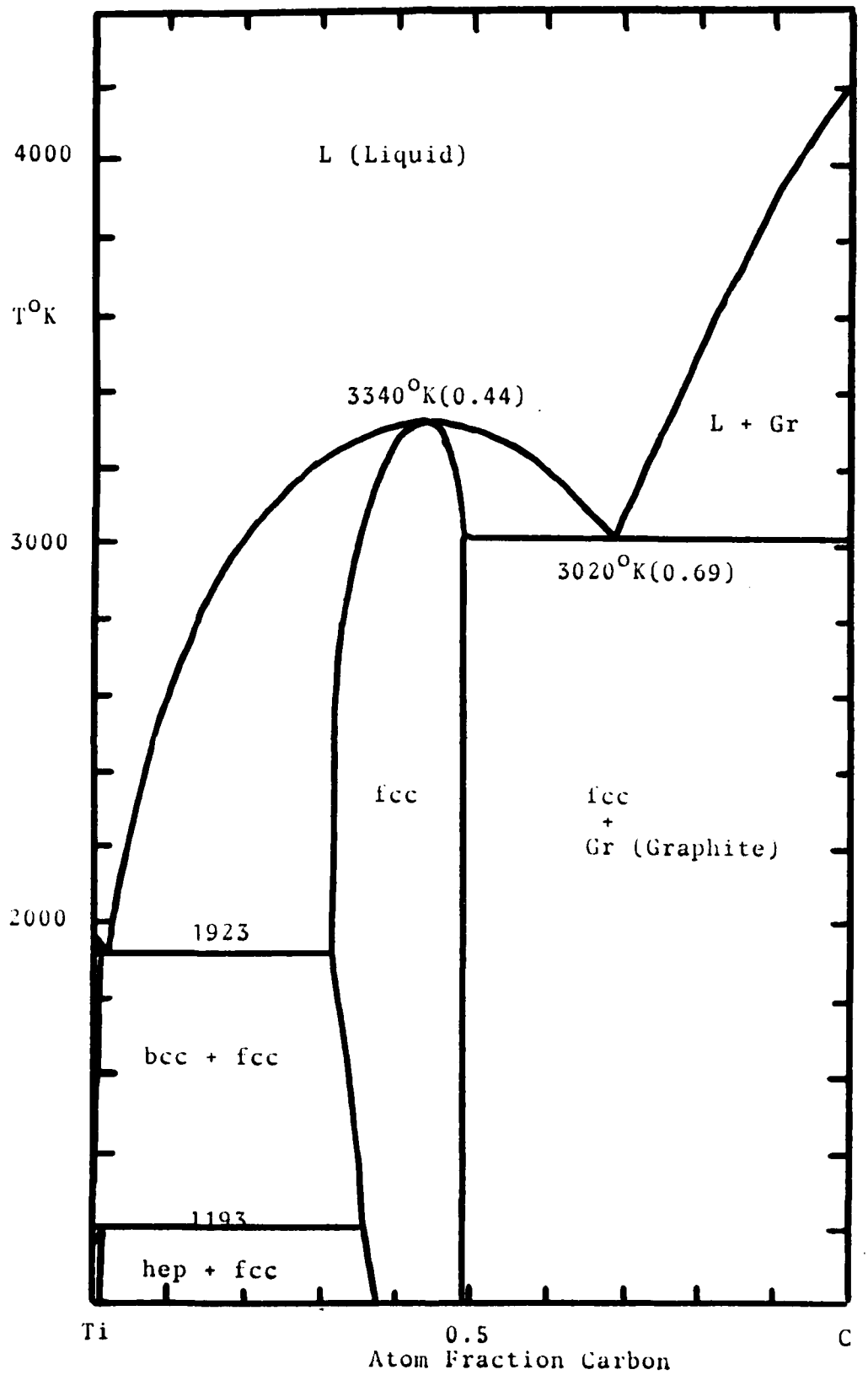

Figure 5. Calculated Titanium-Carbon Phase Diagram

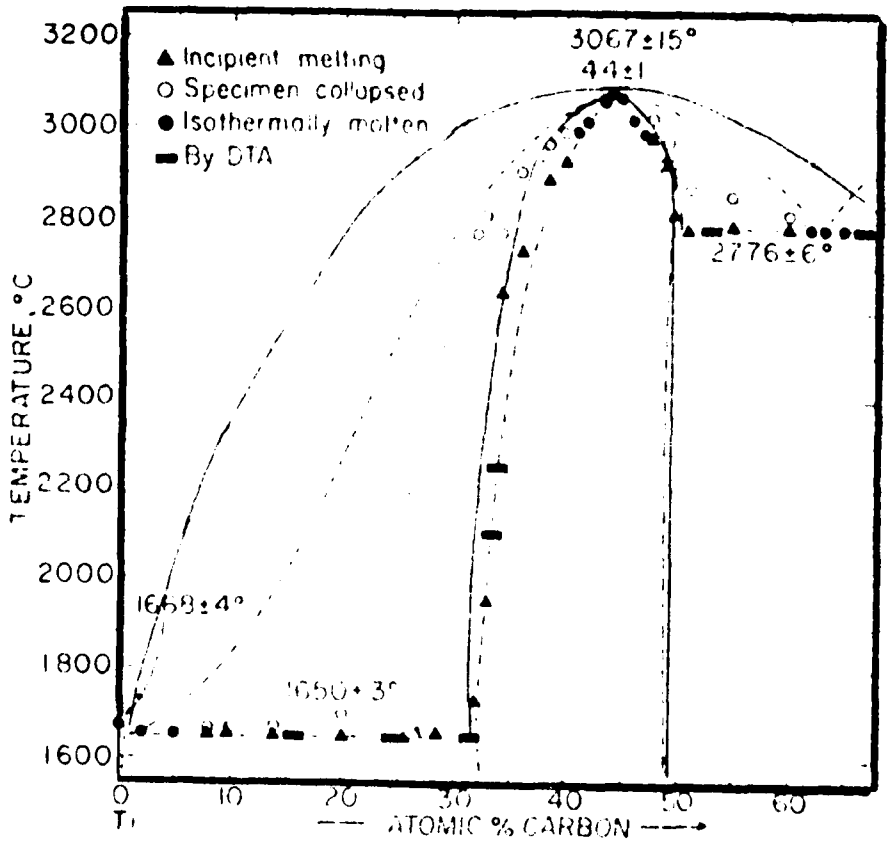

Figure 6. Liquid-Fcc Equilibrium in the Titanium-Carbon System. Solid Curves are calculated. Dashed Curves and Experimental Points are from Reference 9.

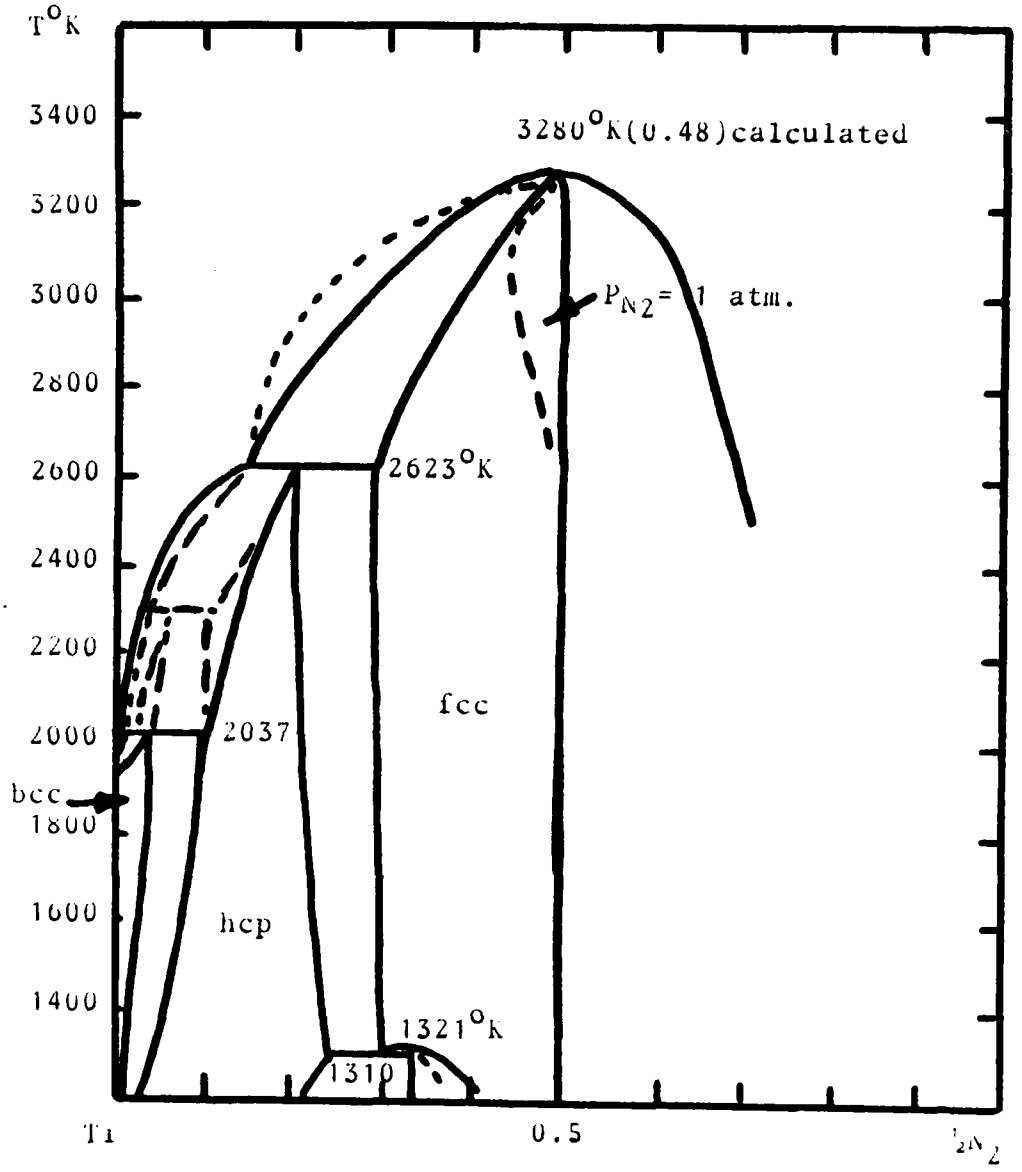

Figure 7. Titanium-Nitrogen Phase Diagram, Solid Curves are calculated, Dashed Curves are after Hultgren Reference 4.

In Hultgren's diagram it is around 2293K (2020 ^{o}C) whereas the calculation yielded 2037k (1764^{o}C). It is easily demonstrated that this part of Hultgren's diagram cannot be self consistent since close to the edges of a phase-diagram the width of a two-phase field is approximately given by $\Delta G/RT$, where ΔG is the free energy difference between the two phases for the solvent (i.e. Ti in this case). At 2293K we have for the width of the L/bcc-field,: $\Delta G/RT = 0.15$, whereas Hultgrens diagram yields about 0.02. A two-phase field which is wider than 0.02 will tend to push the three-phase equilibrium to lower temperature. Altering the width of the two-phase field by changing solution phase parameters cannot be done realistically because the nitrogen concentration in the liquid is too low. It might instead be possible to change the description of the bcc phase but the N-concentration in that is also rather low and non-realistic values are required to obtain agreement with Hultgren. In the latter case one also has to change the hcp and fcc-phases if one wants to keep the agreement with the solid-phase equilibria in the reported phase diagram.

.0 Calculation of Ternary Sections in the Ti-C-N system

In general calculation of the Ti-C-N system requires description of the C-N binary in addition to the Ti-C and Ti-N binaries discussed above. However, since the information required to evaluate such C-N interactions is not available, they were assumed to be equal to zero as a first approximation. On this basis the ternary sections at 1600,1800 and 2500K for the N-C-Ti system shown in Figures 8,9,10 were calculated. The calculation shows that the fcc-field extends from the TiC to the TiN side and that the hcp phase disolves very little carbon.

8.0 Vapor deposition of solid $Ti_{(1-x-y)}C_xN_y$

From a practical point of view it is interesting to determine what composition an input gas must have in order to yield a specific composition x,y of the carbo-nitride. The limiting values at 1800K in the binary Ti-C system, using a mixture of $TiCl_4$, CH_4 and H_2 of P_{tot} = 1 atm, was calculated by Bernard et. al. (12). In principle their calculation could

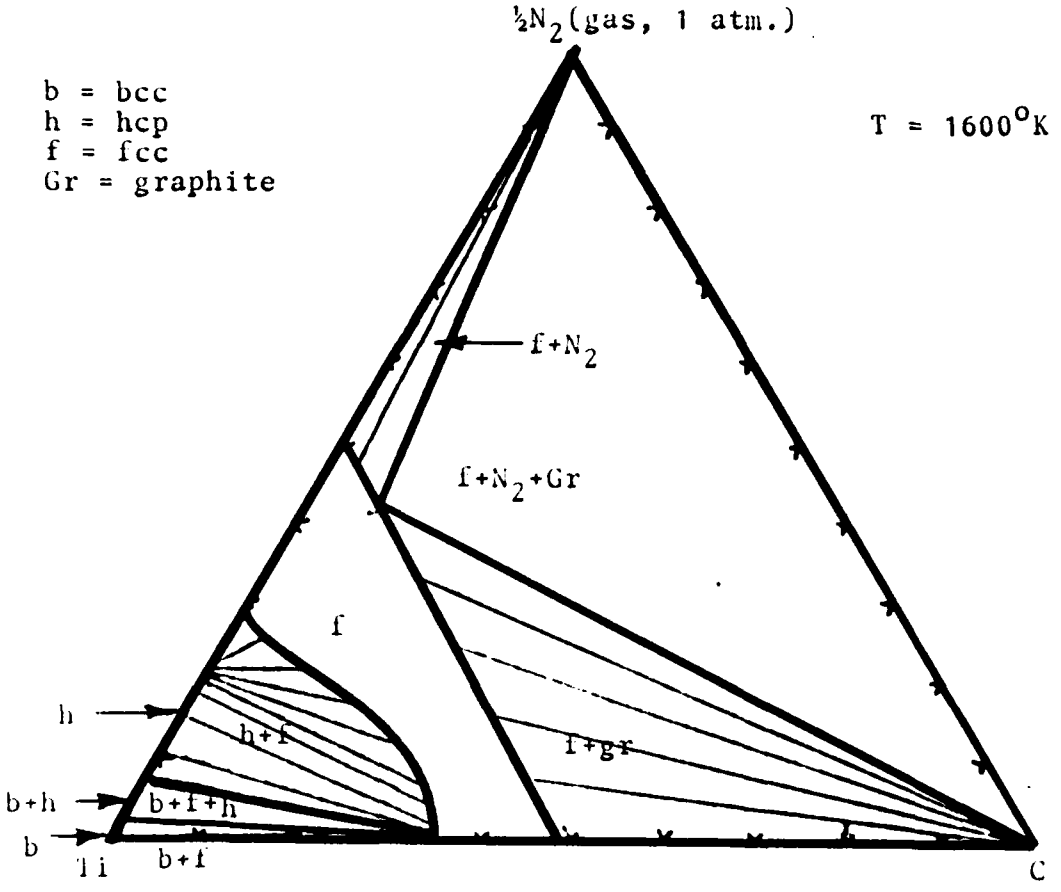

Figure 8. Calculated Isothermal Section at 1600°K in the Titanium-Carbon-Nitrogen System.

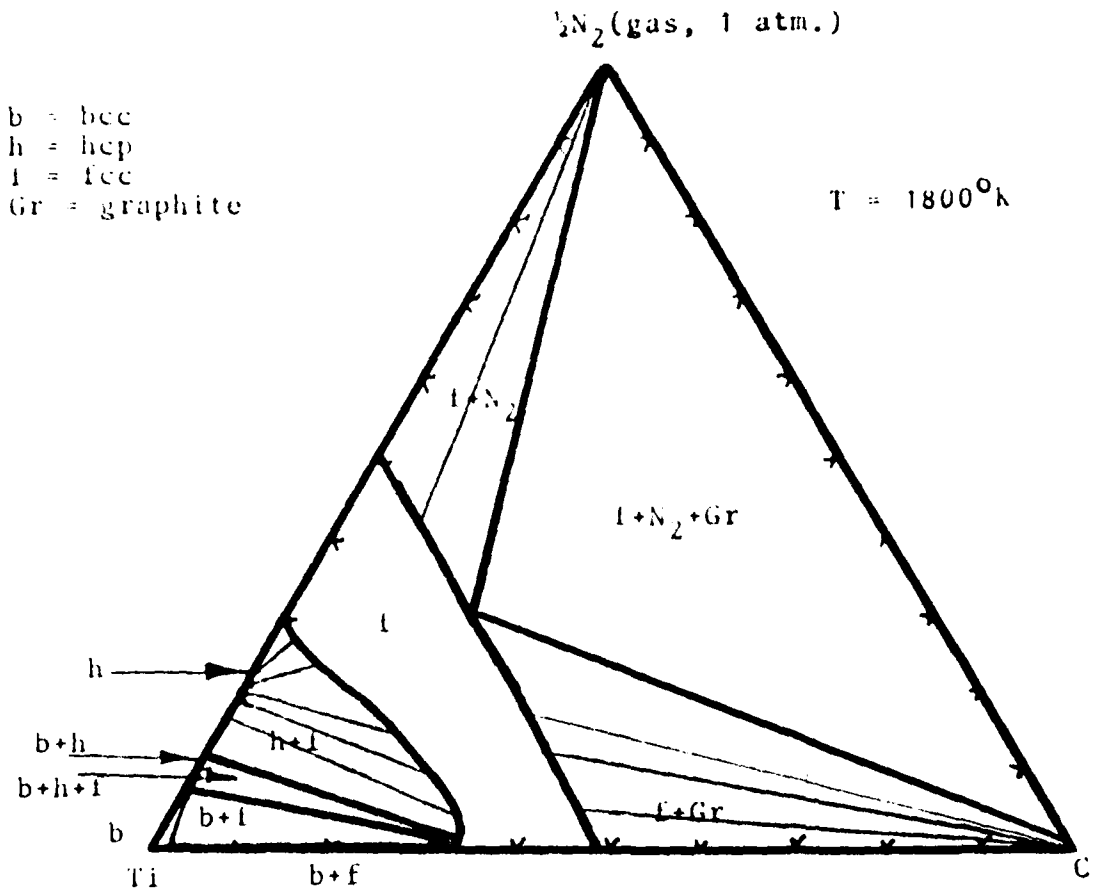

Figure 9. Calculated Isothermal Section in the Titanium-Carbon-Nitrogen System at 1800°K

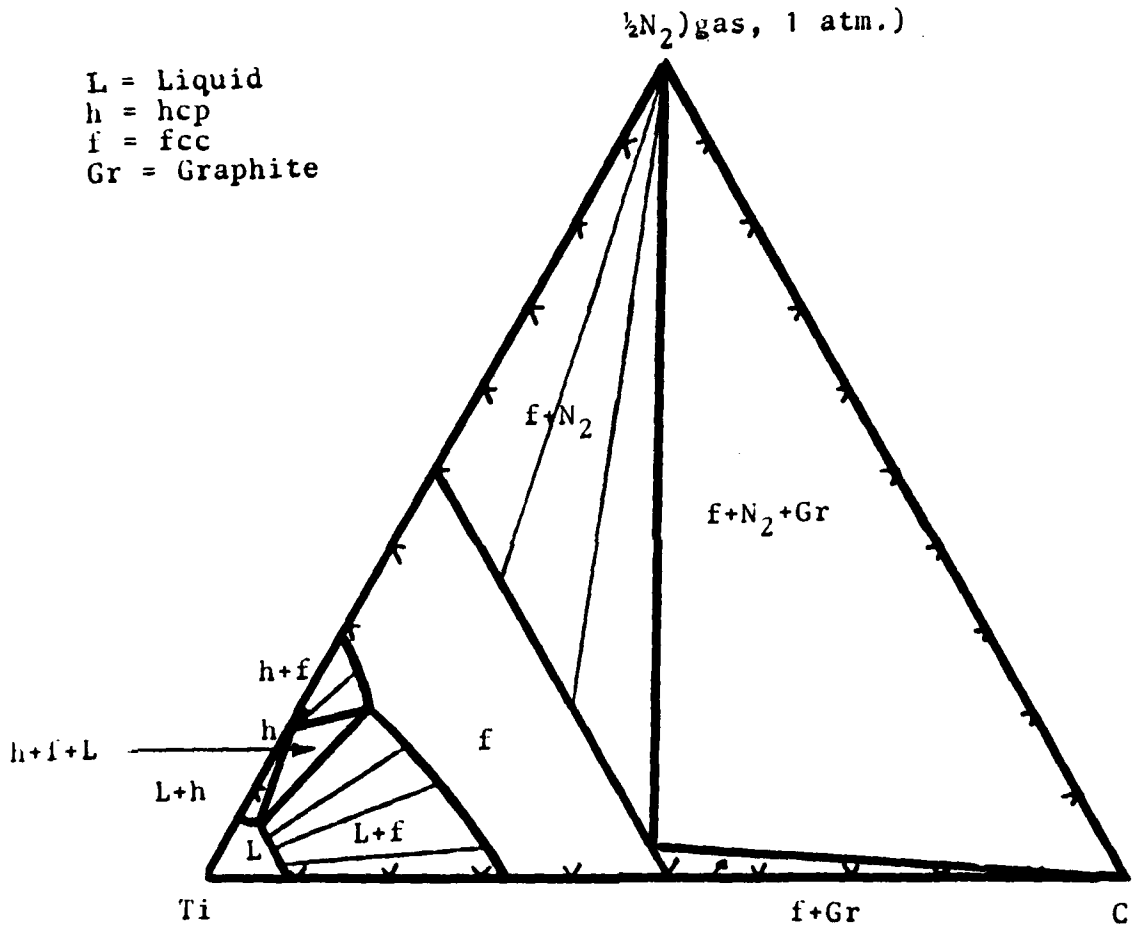

Figure 10. Calculated Isothermal Section in the Titonium-Carbon-Nitrogen System at 2500°K

be repeated not only for the extreme compositions (corresponding to equilibrium with graphite and almost a pure Ti respectively) but for a whole family of different compositions. Each composition would be represented as a curve in the $P^{o}_{TiCl_4}$ - $P^{o}_{CH_4}$ - plot. The calculation is quite straight forward. From the given solid phase composition the C- and Ti-activities can be calculated. By keeping these activities and the total gas-pressure fixed and solving the non-linear system of equations formed by equilibrium and stoichiometric conditions for the gas-mixture one obtains $P^{o}_{TiCl_4}$ when $P^{o}_{CH_4}$ is specified or vice versa. If a nitrogen-bearing component, e.g. NH_3, is added to the input-gas the deposited phase will also contain some N. The input-gas composition required to obtain a certain solid-phase composition is calculated in the same way as in the binary case. From the solid phase compositon the C-, N- and Ti-activities are calculated and the values obtained are inserted to the equilibrium and stoichiometric conditions. In this case, however, each solid phase composition is not represented by a curve in the $P^{o}_{TiCl_4}$ - $P^{o}_{CH_4}$ - plot, but by a surface in the $P^{o}_{TiCl_4}$ - $P^{o}_{CH_4}$ - $P^{o}_{NH_3}$ - plot. In Figures 11-13 the calculated iso-activity lines in the fcc-phase have been ploted for each component at 1800K so that the activities can be estimated easily for a certain composition at this temperature. As expected, the nitrogen and carbon activities required to obtain a solid phase without vacancies, i.e. $x_{Ti} = 0.5$, are infinitely high.

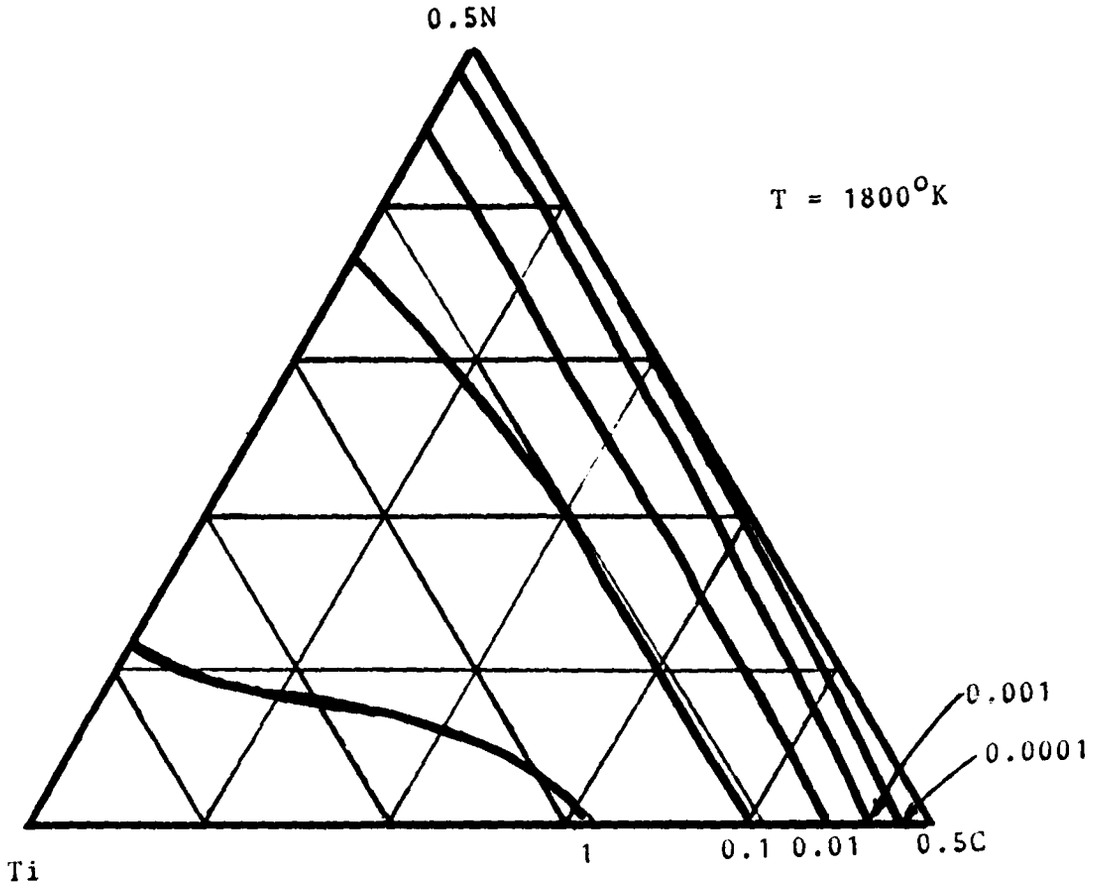

Figure 11. Calculated Iso-activity lines for Titonium in Ti(C,N) at 1800K

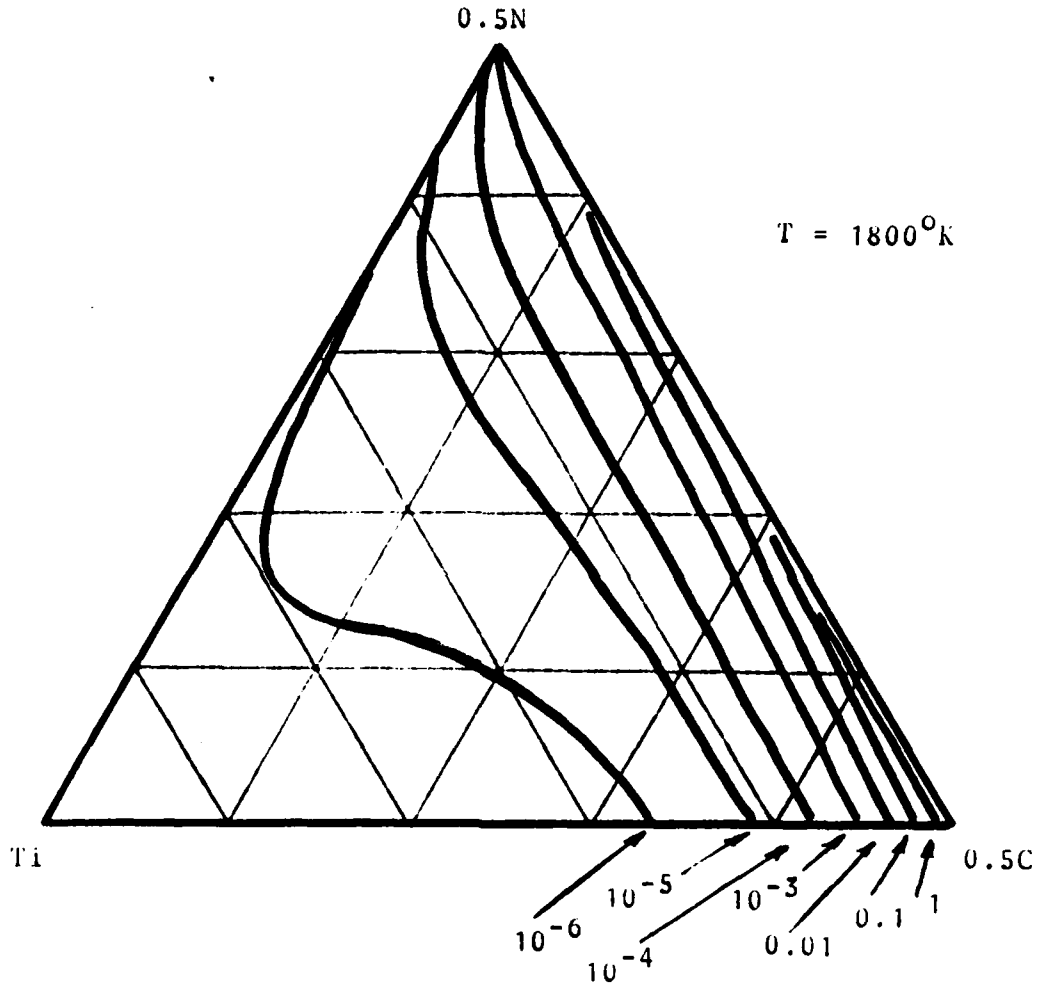

Figure 12. Calculated Iso-activity lines for carbon in Ti(N,C) at 1800°K

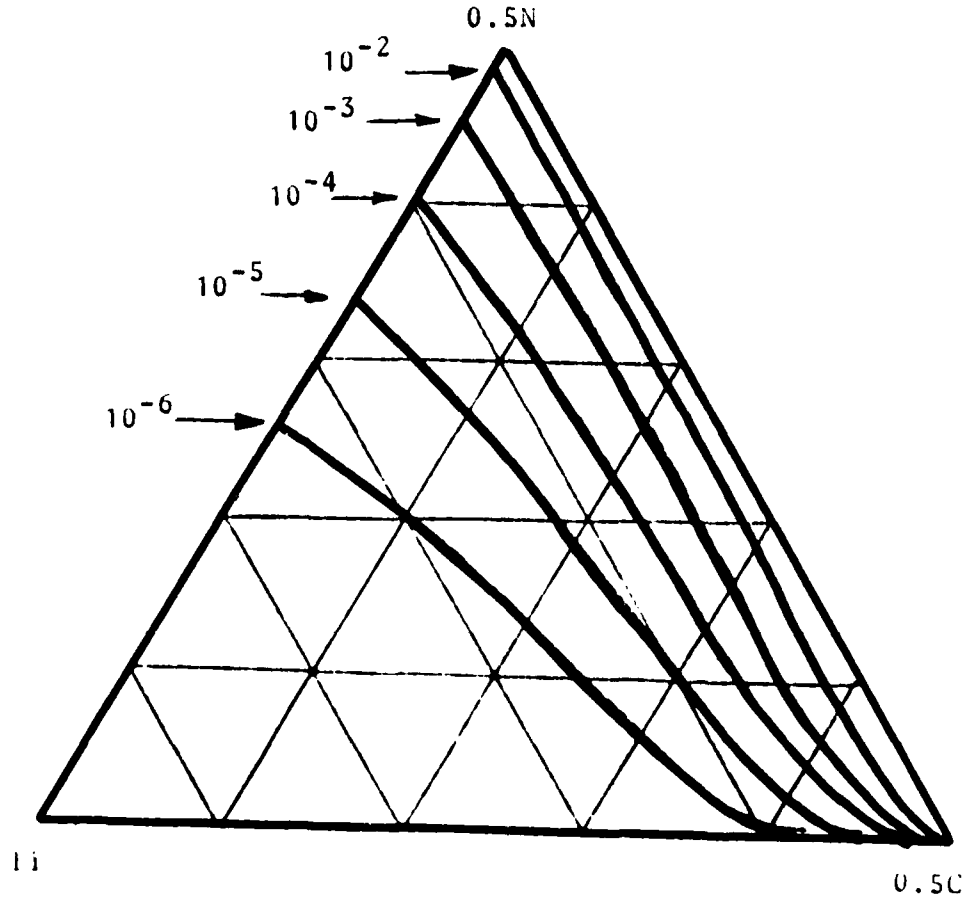

Figure 13. Calculated iso-activity lines for N (i.e. $\frac{1}{2}N_2$) at 1800K in Ti(C,N).

Appendix

For a ternary regular solution we apply the following equation for the integral Gibbs energy:

$$G_m = x_A {}^oG_A + x_B {}^oG_B + x_C {}^oG_C + RT\left[x_A \ln x_A + x_B \ln x_B + x_C \ln x_C\right] + x_A x_B L_{AB} + x_A x_C L_{AC} + x_B x_C L_{BC} \quad (A1)$$

where x_A, x_B, x_C are the molar fractions and subjected to the condition :

$$x_A + x_B + x_C = 1 \quad (A2)$$

${}^oG_A$, ${}^oG_B$, ${}^oG_C$ are the Gibbs energies for the pure components in the phase under consideration, and L_{AB}, L_{AC}, L_{BC} are interaction-parameters. In a subregular solution the interaction parameters exhibit a linear concentration dependence in the binary edge-systems. In this report the following representation has been applied in the binaries:

$$L_{AB} = {}^oL_{AB} + {}^1L_{AB}(x_A - x_B) \quad (A3)$$

The same representation will also be applied for a ternary solution. By standard methods the partial quantities are derived:

$$G_j = {}^oG_j + RT \ln x_j + {}^EG_j \qquad j = A,B,C \quad (A4)$$

where

$$\begin{aligned} {}^EG_A = {} & x_B(1-x_A) {}^oL_{AB} + \left[x_B^2 + 2x_B(1-x_A)(x_A-x_B)\right] {}^1L_{AB} \\ & + x_C(1-x_A) {}^oL_{AC} + \left[x_C^2 + 2x_C(1-x_A)(x_A-x_C)\right] {}^1L_{AC} \\ & - x_B x_C {}^oL_{BC} - 2x_B x_C (x_B - x_C) {}^1L_{BC} \end{aligned} \quad (A5)$$

$$\begin{aligned} {}^EG_B = {} & x_A(1-x_B) {}^oL_{AB} - \left[x_A^2 - 2x_A(1-x_B)(x_A-x_B)\right] {}^1L_{AB} + \\ & + x_C(1-x_B) {}^oL_{BC} + \left[x_C^2 + 2x_C(1-x_B)(x_B-x_C)\right] {}^1L_{BC} \\ & - x_A x_C {}^oL_{AC} - 2x_A x_C (x_A - x_C) {}^1L_{AC} \end{aligned} \quad (A6)$$

$$\begin{aligned} {}^EG_C = {} & x_A(1-x_C) {}^oL_{AC} - \left[x_A^2 - 2x_A(1-x_C)(x_A-x_C)\right] {}^1L_{AC} \\ & + x_B(1-x_C) {}^oL_{BC} - \left[x_B^2 - 2x_B(1-x_C)(x_B-x_C)\right] {}^1L_{BC} \\ & - x_A x_B {}^oL_{AB} - 2x_A x_B (x_A - x_B) {}^1L_{AB} \end{aligned} \quad (A7)$$

The sublattice model takes the following form for the case of Ti on one sublattice and a mixture of C, N and Va (=vacant sites) on the other sublattice (i.e. $Ti_a (C,N,Va)_c$)

$$G_m = y_C {}^oG_{Ti_aC_c} + y_N {}^oG_{Ti_aN_c} + y_{Va} {}^aG_{Ti}$$
$$+ RT\, c \left[y_C \ln y_C + y_N \ln y_N + y_{Va} \ln y_{Va} \right]$$
$$+ y_C y_N L^{Ti}_{CN} + y_C y_{Va} L^{Ti}_{CVa}$$
$$+ y_N y_{Va} L^{Ti}_{NVa} \qquad (A8)$$

where the site fractions, y can be calculated from the ordinary mole fractions by the equations:

$$y_C = \frac{a}{c} x_C/(1-x_C - x_N) \qquad (A9)$$

$$y_N = \frac{a}{c} x_N/(1-x_C - x_N) \qquad (A10)$$

$$\text{and } y_{Va} = 1-y_C - y_N \qquad (A11)$$

The subscript m in equation A8 signifies that G is counted per mole of formula unit: $Ti_a(C,N,Va)_c$. In order to compute G for a mole of atoms (or a gram atom) equation A8 must be multiplied by the factor $(1/a)\ (1-x_N-x_C)$. The following values of a and c hold:

fcc: a=1, c=1
bcc: a=1, c=3
hcp: a=2, c=1 (A12)

${}^oG_{Ti_aC_c}$ and ${}^oG_{Ti_aN_c}$ are the Gibbs energy of formation for the compounds. These compounds may or may not be stable. Moreover, experimental data may or may not be available for the compounds.

The L-parameters are interaction parameters and are defined to vary with composition as:

$$L_{ij} = {}^oL_{ij} + {}^1L_{ij}\ (y_i - y_j) \qquad (A13)$$

The partial quantities become:

$$G_C = \frac{1}{c}\left({}^{o}G_{Ti_aC_c} - a\,{}^{o}G_{Ti}\right) + RT\left(\ln y_C - \ln y_{Va}\right) + {}^{E}G_C$$

$$G_N = \frac{1}{c}\left({}^{o}G_{Ti_aN_c} - a\,{}^{o}G_{Ti}\right) + RT\left(\ln y - \ln y_{Va}\right) + {}^{E}G_N$$

$$G_{Ti} = {}^{o}G_{Ti} + RT\,\frac{c}{a}\ln Y_{Va} + {}^{E}G_{Ti}$$

Furthermore;

$${}^{E}G_C = \frac{1}{c}\left({}^{E}G_{Ti_aC_c} - {}^{E}G_{Ti_aVa_c}\right) \qquad (A13)$$

$${}^{E}G_N = \frac{1}{c}\left({}^{E}G_{Ti_aN_c} - {}^{E}G_{Ti_aVa_c}\right) \qquad (A14)$$

$${}^{E}G_{Ti} = \frac{1}{a}\,{}^{E}G_{Ti_aVa_c} \qquad (A15)$$

and

$${}^{E}G_{Ti_aC_c} = y_N(1-y_C)\,{}^{o}L^{Ti}_{CN} + \left[y_N^2 + 2y_N(1-y_C)(y_C-y_N)\right]{}^{1}L^{Ti}_{CN} + y_{Va}(1-y_C)\,{}^{o}L^{Ti}_{CVa} + \left[y_{Va}^2 + 2y_{Va}(1-y_C)(y_C-y_{Va})\right]{}^{1}L^{Ti}_{CVa} - y_Ny_{Va}\,{}^{o}L^{Ti}_{NVa} - 2y_Ny_{Va}(y_N-y_{Va})\,{}^{1}L^{Ti}_{NVa} \qquad (A16)$$

$${}^{E}G_{Ti_aN_C} = y_C(1-y_N)\,{}^{o}L^{Ti}_{CN} - \left[y_C^2 - 2y_C(1-y_N)(y_C-y_N)\right]{}^{1}L^{Ti}_{CN} + y_{Va}(1-y_N)\,{}^{o}L^{Ti}_{NVa} + \left[y_{Va}^2 + 2y_{Va}(1-y_N)(y_N-y_{Va})\right]{}^{1}L^{Ti}_{NVa} - y_Cy_{Va}\,{}^{o}L^{Ti}_{CVa} - 2y_Cy_{Va}(y_C-y_{Va})\,{}^{1}L^{Ti}_{CVa} \qquad (A17)$$

$${}^{E}G_{Ti_aVa_c} = y_C(1-y_{Va})\,{}^{o}L^{Ti}_{CVa} - \left[y_C^2 - 2y_C(1-y_{Va})(y_C-y_{Va})\right]{}^{1}L^{Ti}_{CVa} + y_N(1-y_{Va})\,{}^{o}L^{Ti}_{NVa} - \left[y_N^2 - 2y_N(1-y_{Va})(y_N-y_{Va})\right]{}^{1}L^{Ti}_{NVa} - y_Cy_N\,{}^{o}L^{Va}_{CN} - 2y_Cy_N(y_C-y_N)\,{}^{1}L^{Ti}_{CN} \qquad (A18)$$

Appendix C

Summary of parameters for Ti-C-N system. (cal/mol, conversion to J/mol by multiplying by 4.184).

Liquid

$${}^{o}G^{L}_{Ti} - {}^{o}G^{hcp}_{Ti} = 4920 - 2.9T \qquad \text{(Ref. 8)}$$

$${}^{o}G^{L}_{C} - {}^{o}G^{gr}_{C} = 27300 - 6.5T \qquad \text{-11-}$$

$${}^{o}G^{L}_{N} - \frac{1}{2}\,{}^{o}G^{gas}_{N_2} = -2077 + 15.98T \qquad \text{-11-}$$

Subregular solution, G_m given by Eq. A1.

$${}^{o}L^{L}_{CN} = {}^{1}L^{L}_{CN} = 0$$

$${}^{o}L^{L}_{CTi} = -23185 - 10.5T,\ {}^{1}L^{L}_{CTi} = 30516 - 10.5T$$

$${}^{o}L^{L}_{NTi} = -68482 - 7.5T,\ {}^{1}L^{L}_{NTi} = 40975 + 7.5T$$

fcc

$${}^{o}G^{fcc}_{Ti} - {}^{o}G^{hcp}_{Ti} = 800 \qquad \text{(Ref. 8)}$$

$${}^{o}G^{fcc}_{TiC} - {}^{o}G^{hcp}_{Ti} - {}^{o}G^{Gr}_{C} = -43972 + 2.528T$$

$${}^{o}G^{fcc}_{TiN} - {}^{o}G^{hcp}_{Ti} - \frac{1}{2}\,{}^{o}G^{gas}_{N_2} = -79666 + 21.42T$$

Sublattice model, G_m given by Eq. A8 a=c=1

$${}^{o}L^{Tifcc}_{CN} = {}^{1}L^{Tifcc}_{CN} = 0$$

$${}^{o}L^{Tifcc}_{CVa} = -16099 + 0.36T,\ {}^{1}L^{Tifcc}_{CVa} = -38801 + 11.03T$$

$${}^{o}L^{Tifcc}_{NVa} = -25000 + 4.4T,\ {}^{1}L^{Tifcc}_{NVA} = 0$$

hcp

Ref state for Ti

$${}^{o}G^{hcp}_{Ti_2C} - 2\,{}^{o}G^{hcp}_{Ti} - {}^{o}G^{Gr}_{C} = 5574$$

$${}^{o}G^{hcp}_{Ti_2N} - 2\,{}^{o}G^{hcp}_{Ti} - \frac{1}{2}\,{}^{o}G^{gas}_{N_2} = -93490 + 24.71T$$

sublattice model, G_m given by Eq. A8 a = 2, c = 1

$${}^{o}L^{Tihcp}_{CN} = {}^{1}L^{Tihcp}_{CN} = 0$$

$${}^{o}L^{Tihcp}_{CVa} = -50000, \quad {}^{1}L^{Tihcp}_{CVa} = 0$$

$${}^{o}L^{Tihcp}_{NVa} = -9985 - 3.44T, \quad {}^{1}L^{Tihcp}_{NVa} = 0$$

bcc

$${}^{o}G^{bcc}_{Ti} - {}^{o}G^{hcp}_{Ti} = 1040 - 0.9T$$

$${}^{o}G^{bcc}_{TiC_3} - {}^{o}G^{hcp}_{Ti} - 3\,{}^{o}G^{gr}_{C} = -44996 + 0.49T$$

$${}^{o}G^{bcc}_{TiN_3} - {}^{o}G^{hcp}_{Ti} - 3/2\,{}^{o}G^{gas}_{N_2} = -104155 + 31.22T$$

sublattice model, G_m given by Eq. A8 a = 1, c = 3

$${}^{o}L^{Tibcc}_{CN} = {}^{1}L^{Tibcc}_{CN} = 0$$

$${}^{o}L^{Tibcc}_{CVa} = -50000, \quad {}^{1}L^{Tibcc}_{CVa} = 0$$

$${}^{o}L^{Tibcc}_{NVa} = {}^{1}L^{Tibcc}_{NVa} = 0$$

Tetragonal

$${}^{o}G^{tet}_{Ti_2N} - 2\,{}^{o}G^{hcp}_{Ti} - \frac{1}{2}\,{}^{o}G^{gas}_{N_2} = -120692 + 43.06T$$

Stoichiometric Phase

Gas $\quad {}^{o}G^{gas}_{Ti} - {}^{o}G^{hcp}_{Ti} = 112685 - 48.024T + 1.808\,T\ln T$ (Ref. 6)

REFERENCES

1. R.C. Sharma and Y.A. Chang: Metall Trans. B, 10 B (1979) pp 103-108.

2. A. Fernandez Guillermet, M. Hillert, B. Jansson and B. Sundman: Metall Trans. B, 12B (1981) pp. 745-754

3. R. Hultgren et. al: Selected Values of the Thermodynamic Properties of Metals (and Binary Alloys), (2 volumes) ASM, Metals Park, Ohio 1973.

4. M. Hillert and L. I. Staffansson: Acta Chem Scand. 24 (1970) pp 3618-26.

5. B. Sundman and J. Agren: J. Phys. Chem. Solids, 42 (1981) pp 297-301

6. J. Agren: Metall. Trans, A, 10A (1979) pp 1847-52.

7. O Kubaschewski and C.B. Alcock: Metallurgical Thermochemistry, 5th edition, Pergamon Press, Oxford 1979.

8. E.K. Storms: Refractory Carbides Academic Press, New York 1967.

9. L. Kaufman: CALPHAD I (1977) P.7

10. E. Rudy, D.P. Harmon, and C.E. Brukl (1965) Wright-Patterson Air Force Base Tech. Rept. No AFML-TR-65-2, Part 1 Volume II.

11. M. Hansen and K. Anderko: Constitution of Binary Alloys 2nd Edition, McGraw Hill 1958.

12. F. Teyssandier, M. Ducarroir and C. Bernard: The Industrial Use of Thermochemical Data, pp 301-311, Edited by T.I. Barry, The chemical Society, special publication No. 34 London 1980.

DISTRIBUTION LIST Materials

AFOSR/NE
Dr. A.H. Rosenstein
Bolling AFB Washington DC 20332

16 Annual Tech Reports
16 Final Tech Report (1 Draft)
6 Reprints of Each Publication

1 Copy Each:

AFWAL/MLLM
Attn: H. Graham
Wright-Patterson AFB OH 45433

AFWAL/MLLS
Attn: Branch Chief
Wright-Patterson AFB OH 45433

AFWAL/MLLM
Attn: N. Geyer
Wright-Patterson AFB OH 45433

AFWAL/MLLM
Attn: B. Ruh
Wright-Patterson AFB OH 45433

AFWAL/MLLN
Attn: Branch Chief
Wright-Patterson AFB OH 45433

AFWAL/MLBP
Attn: Branch Chief
Wright-Patterson AFB OH 45433

AFWAL/MLBM
Attn: Branch Chief
Wright-Patterson AFB OH 45433

AFWAL/MLLP
Attn: Branch Chief
Wright-Patterson AFB OH 45433

AFWAL/MLPJ
Attn: Branch Chief
Wright-Patterson AFB OH 45433

AFWAL/MLPO
Attn: Branch Chief
Wright-Patterson AFB OH 45433

DARPA
Attn: Lt Col Jacobson
1400 Wilson Blvd
Arlington VA 20339

D.O.E(Material Sciences)
Attn: R.J. Gottschall
Office of Energy Research
Washington DC 20545

Office of Naval Research
Attn: Dr R. Pohanka
800 N. Quincy St.
Arlington VA 22203

U.S. Army Research Office
Metallurgy and Materials Sciences
P.O. Box 12211
Research Triangle Park NC 27709

U.S. Naval Air Systems Command
Attn: Mr. I Machlin (AIR 52031B)
Washington DC 20360

U.S. Naval Research Laboratory
Attn: Dr. R.W. Rice, Chem Div (6360)
Washington DC 20375

NASA-Lewis
Attn: H.B. Probst (Stop 49-3)
21000 Brookpark Rd.
Cleveland OH 44135

J.A. Carpenter Jr
Oak Ridge National Lab
Oak Ridge TN 37830

National Bureau of Standards
Attn: S.M. Wiederhorn
Washington DC 20234

N.S.F. (Materials Research)
Attn: B.A. Wilcox
1800 G Street, N.W.
Washington DC 20550

Materials Research Lab (AMMRC)
Attn: Dr R.N. Katz
Watertown MA 02172

DOE Fossil Energy Div
Dr S.R. Skaggs
FE-3/C-156 Germantown
Washington DC 20544

Dr F.F. Lange
Rockwell International Science Center
Thousand Oaks CA 91360r)

Dr A.H. Heuer
Dept of Material Science
Case Western Reserve University
Cleveland OH 43201

Dr G.H. Meier
Dr F.S. Pettit
Metallurigical and Materials Engineering
University of Pittsburgh
Pittsburgh PA 15261

Dr. L. Kaufman
ManLabs, Inc.
21 Erie St.
Cambridge, MA 02139

Dr I. Allam
SRI Internationl
333 Ravenswood Ave
Menlo Park CA 94025

Dr D. Rowcliff
SRI International
333 Ravenswood Ave.
Menlo Park, CA 94025

Dr Roger R. Wills
Section Manager, Ceramics and
Materials Processing Section
Battelle Columbus Labs
Columbus OH 43201

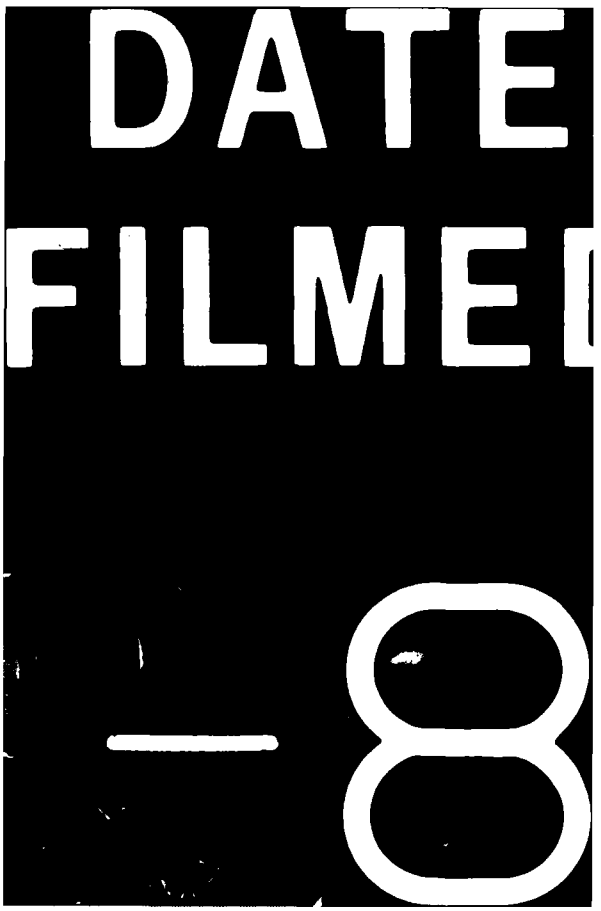
DATE
FILME
8